

RESEARCH ARTICLE

Comparison of the secretory murine DNase1 family members expressed in *Pichia pastoris*

Lukas Verhülsdonk¹, Hans Georg Mannherz^{1,2}, Markus Napirei^{1*}

1 Department of Anatomy and Molecular Embryology, Medical Faculty, Ruhr-University Bochum, Bochum, Germany, **2** Molecular and Experimental Cardiology, St. Josef-Hospital, Clinics of the Ruhr University Bochum, Bochum, Germany

* markus.napirei@ruhr-uni-bochum.de



Abstract

Soluble nucleases of the deoxyribonuclease 1 (DNase1) family facilitate DNA and chromatin disposal (chromatinolysis) during certain forms of cell differentiation and death and participate in the suppression of anti-nuclear autoimmunity as well as thrombotic microangiopathies caused by aggregated neutrophil extracellular traps. Since a systematic and direct comparison of the specific activities and properties of the secretory DNase1 family members is still missing, we expressed and purified recombinant murine DNase1 (rmDNase1), DNase1-like 2 (rmDNase1L2) and DNase1-like 3 (rmDNase1L3) using *Pichia pastoris*. Employing different strategies for optimizing culture and purification conditions, we achieved yields of pure protein between ~3 mg/l (rmDNase1L2 and rmDNase1L3) and ~9 mg/l (rmDNase1) expression medium. Furthermore, we established a procedure for post-expressional maturation of pre-mature DNase still bound to an unprocessed tri-N-glycosylated pro-peptide of the yeast α -mating factor. We analyzed glycosylation profiles and determined specific DNase activities by the hyperchromicity assay. Additionally, we evaluated substrate specificities under various conditions at equimolar DNase isoform concentrations by lambda DNA and chromatin digestion assays in the presence and absence of heparin and monomeric skeletal muscle α -actin. Our results suggest that due to its biochemical properties rmDNase1L2 can be regarded as an evolutionary intermediate isoform of mDNase1 and mDNase1L3. Consequently, our data show that the secretory DNase1 family members complement each other to achieve optimal DNA degradation and chromatinolysis under a broad spectrum of biological conditions.

OPEN ACCESS

Citation: Verhülsdonk L, Mannherz HG, Napirei M (2021) Comparison of the secretory murine DNase1 family members expressed in *Pichia pastoris*. PLoS ONE 16(7): e0253476. <https://doi.org/10.1371/journal.pone.0253476>

Editor: Israel Silman, Weizmann Institute of Science, ISRAEL

Received: December 2, 2020

Accepted: June 7, 2021

Published: July 30, 2021

Copyright: © 2021 Verhülsdonk et al. This is an open access article distributed under the terms of the [Creative Commons Attribution License](https://creativecommons.org/licenses/by/4.0/), which permits unrestricted use, distribution, and reproduction in any medium, provided the original author and source are credited.

Data Availability Statement: The minimal data set is part of the [supplementary information](#).

Funding: The present work was supported by a grant of the M.D. program of FoRUM (Forschungsförderung, Ruhr-Universität Bochum, Medizin) for Lukas Verhülsdonk. We acknowledge support by the Open Access Publication Funds of the Ruhr-Universität Bochum.

Competing interests: The authors have declared that no competing interests exist.

Introduction

Deoxyriboendonucleases play an important role in the intra- and extracellular clearance of DNA and chromatin during physiological processes such as cell differentiation, programmed cell death, necrosis and NETosis. The DNase1 family consists of DNase1 (also called DNase I) and its three relatives DNase1-like 1–3 which are involved in specific situations of the aforementioned processes [1]. Identified in 1946 and characterized subsequently, DNase1 is regarded as the first known member of the DNase1 family, while its highly homologous

relatives were discovered only later [2]. They share common properties with DNase1 such as the N-terminal signal peptide (SP) for translation into the rough endoplasmic reticulum (rER), the divalent metal cation dependency and the endonucleolytic DNA cleavage activity generating 3'-hydroxyl and 5'-phosphate ends (Fig 1A) [3–7].

The different DNase1-like proteins display specific and partially overlapping expression profiles. Whereas DNase1L1 (also called DNase1L, Xib, DNase X [1]) is a muscle specific and membrane-bound protein, which supposedly builds a barrier against the endocytosis of foreign DNA [18–20], the other three nucleases are soluble secretory proteins, here referred to as the secretory DNase1 family members [7]. The expression pattern of DNase1L2 is restricted to keratinocytes, where it facilitates the removal of genomic DNA during their differentiation to hairs and nails and participates in the cornification process within the epidermis [21, 22]. The broadest expression profile displays DNase1, which occurs in almost all mammalian body fluids and secretions such as tear fluid, saliva, blood, urine, and seminal fluid [23, 24]. The majority of published studies indicate a suppressive function of DNase1 on anti-nuclear autoimmunity, which is typical for Systemic Lupus Erythematosus (SLE) and Lupus-nephritis, the most severe complication of SLE. Indeed, reduced levels of serum and renal DNase1, increased levels of DNase1 inhibitors and *DNASE1/Dnase1* gene mutations were described for humans and mice suffering from SLE [25–30]. It was noted, however, that the SLE phenotype found in the first described *Dnase1* KO mice of mixed 129xBL/6J F2 genetic background depended on additional pre-disposing genes and/or environmental factors, since it does not occur in pure 129 or C57BL/6J mice under specific pathogen-free conditions [31, 32]. Furthermore, the primary *Dnase1* KO mouse model harbored an aberrant knockdown mutation in the overlapping *Trap1* gene, which encodes for the mitochondrial chaperone Trap1/Hsp75 leading to a lack of detectable Trap1 protein [33, 34]. The influence of Trap1 deficiency on SLE is not clarified so far. On the one hand, newly generated *Dnase1* KO mice without *Trap1* impairment exhibit mild SLE-symptoms spontaneously in C57BL/6 mice [35]. This is in contradiction to the findings described for *Dnase1*^{-/-}/*Trap1*^{m/m} mice of the same genetic background [32]. On the other hand, Trap1 deficiency in *Dnase1*^{-/-}/*Trap1*^{m/m} mice leads to an increased stimulation of immune cells in the same inbred strain [34]. Thus, it remains unclear whether and which additional supporting factors are necessary for the induction of the SLE disease in DNase1 deficient mice, because the overall knowledge points to a multi-factorial origin of SLE [31]. In summary, most of the findings suggest that impaired DNase1 activity modifies anti-DNA autoimmunity albeit it might not be the sole cause. This view is supported by the fact that DNase1L3 (also called DNase γ , DNase Y, LS-DNase, nh-DNase [1]), which is expressed by macrophages as well as myeloid dendritic cells and occurs in the blood stream in parallel to DNase1 [36–38], is also regarded as a suppressor of anti-nuclear autoimmunity [38–40]. Both serum nucleases share complementary substrate specificities and act collectively in the dissolution of neutrophil extracellular traps (NETs) thereby preventing acute thrombotic microangiopathy during situations of neutrophilia [37, 41, 42]. Additionally, they dissolve genomic DNA within and expelled from primary and secondary necrotic cells [43–47]. Beside their role in extracellular and necrotic chromatin disposal, they were originally regarded as intracellular apoptotic nucleases [48, 49]. Indeed, overexpression of DNase1 in cell lines induces apoptosis accompanied by the typical internucleosomal DNA degradation [50]. However, the inhibitory effect of monomeric actin and the random chromatin cleavage pattern induced by DNase1 in the absence of proteases appear to make a sole involvement of DNase1 in apoptosis unlikely [51, 52]. These contradictory results might be explained by a recent finding demonstrating that overexpression of DNase1 induces a network of apoptotic endonucleases in transfected cells [53]. One of these endonucleases is DNase1L3, which possesses two nuclear localization signals (NLS, Fig 1A) and intrinsic internucleosomal cleavage capacity [16, 54].

A

```

mDNase1      MRY-TGLMGTLLTLVNL--QLAGTLRIAAPNIRTFGETKMSATLSVYFVKILSRDYIA 57 (35)
mDNase1L2   ---MGWPWAPLTAVALGVMGATLRIGAFNVQSFQGNKVSDDPCGSVIAQILAGYDIA 56 (35)
mDNase1L3   MSLHLPASPRLASLLFLILALHDTLRLCSFNVSFGASKKENHEAMDIIVKIKRCDLI 60 (35)
      .          : *          : **: **: **: * . * :          : : * : * :
      .          :          :          :          :          :          :          :          :

mDNase1      VIOEVRDSHLVAVGKLLDELNRDK--PDTYRYVVSEPLGRKSKYKQYLFVYRPDQVSILD 115 (93)
mDNase1L2   LVQEVKDPDLASVLLMEQINRVS--KHEYGFVSSKPLGRDQYKIMYLFVYRKDVASVVK 114 (93)
mDNase1L3   LLMKIKDSSNNICPMLMEKLNNGNSRRSTTYNYVVISRLGRNTRYKQYAFVYKEKLVSVKT 120 (95)
      : : * : *          * : * : *          * : * * . * * * . * * * * * * * :

mDNase1      SYQYDVGEPGNTTSREPAIVKFFSPYTEVQEFVIVPLAAPTEAVSEIDALYDVYLD 175 (153)
mDNase1L2   TYQYRP-----EPAFSSREPFVVKFVSPCATKELVLIPLAAPHQVAEIDALYDVYLD 169 (148)
mDNase1L3   KYHYHYQ-DGDTVFSREPFVWFHSPFTAVKDFVIVPLTPPETSVKIEIDELVDVYTD 179 (154)
      . : * *          * * * * * : * * *          * : * * * * * * * * * * * *

mDNase1      VWQKWGLEDMFMGTFAGCSYVTSSQWSSIRLRTSPIFQWLIPDSATFVLSHHCAY 234 (212)
mDNase1L2   VIDKWNDDMLFLGTFADKRYVKAHDWPSIRLSSEVFVKWLIPDSATFVGNSCAY 228 (207)
mDNase1L3   VRSQWKTENFIIMGTFAGCSYVPPKAWQNI RLRTDPKFWLIGDQETVVKKS SCAY 239 (214)
      * . : *          : : * : * * * * * . * * * * * * * * * * * * :

mDNase1      RIVVAGALLQAAVVPNSAVPFDFQAEYGLSNQLAEAISDPVEVTLRKI----- 284 (262)
mDNase1L2   RIVVSGAHLRRSLKPHASVHNPFQEEFDLQDQALAISSDFPVEVTFKTH----- 278 (257)
mDNase1L3   RIVLCGQEI VNSVPRSSGVDFQKAYDLSEEEALDVSDFPVEFKLQSSRAFTNRRKSV 299 (274)
      * * : *          : : * : * : * * *          * : * * * * * * * * * * :

mDNase1      ----- 284 (262, 29.7 kDa)
mDNase1L2   ----- 278 (257, 29.0 kDa)
mDNase1L3   SLKRRKKGKGRS 310 (285, 33.1 kDa)
    
```

```

signal peptide      (D1: 22aa / D1L2: 21aa / D1L3: 25aa)
S-S-bond            (1st: C101=C104 / essential 2nd: C173=C209)
N-glycosylation     (N-18 / N-106)
Ca2+-binding        (I: D201,T203,T205,T207,D208 / II: D99,D107,F109,E112)
DNA-binding          (central contacts: R9,R41,Y76,R111,N170,Y175,Y211)
catalytic centre    (H134 + E78, D168, N170, H252 + D212)
Mg2+-binding        (IVb: N7, E39, D251)
actin-binding        (H44,D53,Y65,V67,E69,A114)

nuclear localization signal
    
```

B

```

WT αMF-SP      MRFPSIFTAVLFAASSALAAPVTTTEDETAQIPAEAVIGYLDLEGDFDVAVLPPFSSTN 60
pPinkα-HC      MRFPSIFTAVLFAASSALAAPVTTTEDETAQIPAEAVIGYSDLEGDFDVAVLPPFSSTN 60
      *****

WT αMF-SP      NGLLFTTTIASIAAKEEGVSLDKREAEA 89 (9.3 kDa)
pPinkα-HC      NGLLFTTTIASIAAKEEGVSLDKR---- 85 (8.9 kDa)
      *****

pre-peptide        (19 aa, 2 kDa)
pro-peptide        (66 aa, 7 kDa)
di-basic (EA) spacer-peptide (4 aa, 0.4 kDa)

KEX2 site
N-glycosylation
    
```

(*) fully conserved (.) weak similarity (:) strong similarity

Fig 1. Protein alignment and illustration of functional domains and amino acids. (A) Alignment of the secretory mDNase1 family members by Clustal Omega: the multiple sequence alignment tool of EMBL-EBI. The numbering of essential amino acids refers to the mature mDNase1 protein, most of which were discovered for bovine and human DNase1. The length of the pre-mature and mature sequence is indicated in brackets. References: DNase1 disulfide bridges and Ca²⁺-binding [8, 9], DNase1 N-glycosylation [10], DNase1 DNA binding [11, 12], DNase1 catalytic center and Mg²⁺ binding [9, 11, 13, 14], DNase1 actin binding [15], DNase1L3 nuclear localization signals [16], (B) Wild-type *S. cerevisiae* α-mating factor signal prepro-peptide (αMF-SP) in comparison to that in pPinkα-HC of the *PichiaPinkTM pastoris* expression system [17].

<https://doi.org/10.1371/journal.pone.0253476.g001>

So far, extensive research has been conducted to unravel the physiologic functions of single members of the DNase1 variants, however, a comparative quantitative analysis of their

biochemical properties is still missing [1]. Only one study compared all four human DNase1 proteins after expression with His- and Myc-tags, which might, however, interfere with their natural nuclease properties [7]. Furthermore, due to the low amount of recombinant protein produced by transiently transformed eukaryotic cell lines, the specific activities and the DNA substrate cleavage efficiencies of the nucleases were not estimated [7].

In order to address this missing information, i.e. to characterize and compare the nucleases in a quantitative analysis, we expressed the secretory members of the mDNase1 family using the *PichiaPink™ pastoris* expression system [17]. In this system, the secretion of the recombinant protein is regulated by an expression cassette within vector pPink α -HC, which consists of three constituents: the glycerol repressible and methanol inducible *AOX1* promoter, the N-terminal yeast α -mating factor signal prepro-peptide (α MF-SP) and the *CYC1* transcription terminator [55, 56]. The natural α MF-SP consists of a pre-peptide cleaved by a signal peptidase of the rER, a tri-N-glycosylated pro-peptide cleaved by kexin 2 (KEX2), a membrane-bound serine-type endopeptidase of the Golgi apparatus and a di-basic EA-spacer-peptide cleaved by the vacuolar dipeptidyl-aminopeptidase A Ste13. In contrast, the α MF-SP within pPink α -HC lacks the spacer-peptide (Fig 1B). Advantages of this system are an easy and stable transformation with *Ade2* complementation for selection, a high cell density in the expression culture, which should lead to a high expression level, a eukaryotic protein processing including glycosylation allowing the purification of the recombinant protein from the expression culture supernatant (SN) in the absence of excessive foreign protein.

In this manuscript, we describe a systematic optimization of the expression of rmDNase1, rmDNase1L2 and rmDNase1L3 in *P. pastoris* by adapting the culture parameters and conditions. The adjustments ultimately led to an optimized processing of pre-mature α MF-DNases to the mature DNases. Purification procedures for the recombinant nucleases were established and the specific properties and activities under different ionic, pH-value and substrate conditions were quantified and compared.

Materials and methods

Accession numbers

Nucleotide sequence of the *Mus musculus Dnase1* (GenBank No. **NM_010061**), *Dnase12* (GenBank No. **NM_025718.3**) and *Dnase13* mRNA (GenBank No. **NM_007870.3**). Protein sequence of *Mus musculus* DNase1 (UniProtKB—**P49183**), DNase1L2 (UniProtKB—**Q9D1G0**), DNase1L3 (UniProtKB—**O55070**), and of *Saccharomyces cerevisiae* Mating factor alpha-1 (UniProtKB—**P01149**).

Vector constructions for mDNase1

The cDNA encoding pre-mature renal mDNase1 was cloned as done and described in a previous study [37]. For expression in *P. pastoris*, the cDNA encoding mature mDNase1 was amplified using the primer pair Pich-D1-for/rev (Table 1) and cloned between the *StuI-KpnI* sites of pPink α -HC (Invitrogen) in fusion to the N-terminal α MF-SP.

Vector constructions for mDNase1L2 and KEX2

The cDNA encoding pre-mature mDNase1L2 was amplified by RT-PCR using the primer pair D1L2-for2/rev2 (Table 1) and cutaneous RNA of a C57BL/6 mouse. Having been cloned into pJET1.2-blunt (Fermentas), it was reamplified using the same primers and cloned between the *EcoRI-NotI* sites of pDsRed-N1 (Clontech). For expression of mDNase1L2 in *P. pastoris*, the cDNA encoding mature mDNase1L2 was amplified using the primer pair Pich-D1L2-for/rev

Table 1. Primers.

Cloning primers (Eurofins)		Cloned vector
		Cloning sites
D1L2-for2	5' -cagGAATTctgcttttgcATGGGTTGG-3'	pJET1.2/mDNase1L2 blunt-end
D1L2-rev2	5' -CTGTGAacacatttaGCGGCCGccta-3'	pDs/mDNase1L2 EcoRI / NotI
Pich-D1L2-for	5' -CTGCGGATTGGAGCCTTCAATGTTTCAGAG-3'	pPink α -HC/mDNase1L2
Pich-D1L2-rev	5' -ATATCCTGAGGCTGGTACCTCAGTGAG-3'	StuI / KpnI
AOX1-for2	5' -CCCCCTCGACGTCTAACATCCAAAGACGAAAGG-3'	pPink α -HC/mDNase1L2-2x pPink α -HC/mDNase1L2-KEX2
CYC1-rev2	5' -CCGCGGTGACGTCCGCAAATTAAGCCTTCGAGCG-3'	pPink α -HC/mDNase1L2-KEX2-dTM613 pPink α -HC/mDNase1L3-2x AatII
AOX1-for1	5' -GCCAGTGAATTGAGATCTAACATCCAAAG-3'	pPink-HC
AOX1-rev1	5' -GAAGGAAAAGGCCCTCGTTTCGAATAATTAGTTG-3'	BglII / StuI
Pich-SP-D1L2-for	5' -CCTATGGGTTGGCCCTGGGCCCGTGACAG-3'	pPink-HC/SP-mDNase1L2
Pich-SP-D1L2-rev	5' -ATATCCTGAGGCTGGTACCTCAGTGAG-3'	StuI / KpnI
AOX1-for1'	5' -GCCAGTGAATTGAGATCTAACATCCAAAG-3'	pRS415/MeOH-KEX2
AOX1-rev1'	5' -GAAGGAAAAGGCCCTCGTTTCGAATAATTAGTTG-3'	XhoI / PstI
CYC1-for1	5' -CCTTTGTGGATCCCATGTAATTAGTTATGTCAC-3'	pRS415/MeOH-KEX2
CYC1-rev1	5' -CGCGGATCGCGGCCGCAAATTAAGCC-3'	BamHI / NotI
KEX2-for2	5' -CTAACCATCTGCAGATGAAAGTGAGG-3'	pRS415/MeOH-KEX2-dUTR
KEX2-rev2	5' -TTCTGTACGGATCCAAATCAGCATCGTCCGG-3'	PstI / BamHI
KEX2-dTM613-for2	5' -TTCGAAACGCTGCAGATGaaagtgagg-3'	pRS415/MeOH-KEX2-dTM613
KEX2-dTM613-rev2	5' -TGGCCGGCCGGATCCCAACTTCTCAACG-3'	PstI / BamHI
Pich-D1-for	5' -CTGAGAATTGCAGCCTTCAACATTCGG-3'	pPink α -HC/mDNase1
Pich-D1-rev	5' -AACTGCTCAGGTACCTCAGATTTTTCTGAGTG-3'	StuI / KpnI
Pich-D1L3-for	5' -CTAAGGCTCTGCTCCTTCAATGTGAGG-3'	pPink α -HC/mDNase1L3
Pich-D1L3-rev	5' -AAAGGCAGCGGTACCTAGGAGCG-3'	StuI / KpnI
sequencing primers (Eurofins)		
AOX1	5' -GACTGGTTCCAATTGACAAGC-3'	
CYC1	5' -GCGTGAATGTAAGCGTGAC-3'	

<https://doi.org/10.1371/journal.pone.0253476.t001>

(Table 1) and cloned between the *StuI-KpnI* sites of pPink α -HC in fusion to the α MF-SP. For enhanced expression, the expression cassette of pPink α -HC/mDNase1L2 was amplified using the primer pair AOX1-for2/CYC1-rev2 (Table 1) and cloned into the *AatII* site of the same vector to generate pPink α -HC/mDNase1L2-2x. In order to evaluate the expression of mDNase1L2 when tagged to its natural SP, the cDNA encoding pre-mature mDNase1L2 was amplified from pJET1.2/mDNase1L2 using the primer pair Pich-SP-D1L2-for/rev (Table 1) and cloned between the *StuI-KpnI* sites of pPink-HC. In order to generate pPink-HC, the α MF-SP of pPink α -HC was eliminated by *BglII/StuI* cleavage and the 5'-part of the expression cassette was replaced by an amplicon consisting of only the *AOX1* promoter, Kozak sequence and *StuI* site using the primer pair AOX-for1/rev1 (Table 1). For co-expression of α MF-DNase1L2 and KEX2, we first modified pRS415/KEX2 (Addgene, #10996) by generating an expression cassette with *AOX1* promoter and *CYC1* terminator. First, the *AOX1* promoter was amplified from pPink α -HC with primers AOX1-for1'/rev1' (Table 1) and cloned between the *XhoI-PstI* sites and secondly, the *CYC1* terminator was amplified with primers CYC1-for1/rev1 (Table 1) and

cloned between the *Bam*HI-*Not*I sites of pRS415/KEX2 to reach of pRS415/MeOH-KEX2. Next, the 5'- and 3'-UTR of *KEX2* in vector pRS415/MeOH-KEX2 were eliminated by amplifying *KEX2-dUTR* with primers KEX2-for2/rev2 (Table 1) and cloning it between the *Pst*I-*Bam*HI sites of the same vector. For expression of secretory *KEX2* lacking the transmembrane domain [57], a *KEX2* variant coding for the first 613 aa was amplified using the primers KEX2- Δ TM613-for2/rev2 (Table 1) and cloned into the *Pst*I-*Bam*HI sites of vector pRS415/MeOH-KEX2 thereby replacing the full-length *KEX2* cDNA and generating pRS415/MeOH-KEX2- Δ TM613. In order to achieve co-expression of α MF-DNase1L2 and *KEX2* or *KEX2- Δ TM613*, the expression cassettes of the *KEX2* variants were amplified with primers AOX1-for2/CYC1-rev2 (Table 1) from the pRS415 vectors and cloned into the *Aat*II site of pPink α -HC/mdNase1L2.

Vector constructions for mdNase1L3

The cDNA encoding pre-mature splenic mdNase1L3 was cloned as done and described in a previous study except that the reverse primer was inadvertently specified incorrectly [37]. The reverse primer used in the previous study had the sequence 5' -GCGTGATACCTAGGAGCG ATTG-3'. In order to express mdNase1L3 in *P. pastoris*, the cDNA encoding mature mdNase1L3 was amplified using the primer pair Pich-DN1L3-for/rev (Table 1) and cloned between the *Stu*I-*Kpn*I sites of pPink α -HC in fusion to the N-terminal α MF-SP. For enhanced expression, the expression cassette of pPink α -HC/mdNase1L3 was amplified using the primer pair AOX1-for2/CYC1-rev2 (Table 1) and cloned into the *Aat*II site of the same vector to generate pPink α -HC/mdNase1L3-2x.

During revision of the manuscript, we noted retrospectively that the previous *mDnase1l3* cDNA preparation [37] contained two mutations each present in a separate cDNA molecule. First, an A to G substitution of nt-298 and secondly, an A to G substitution of nt-914 (CDS of NM_007870.3 encoding pre-mature mdNase1L3). Mutation nt-298 led to an exchange of Arg (R) to Gly(G)100 in the first NLS of natural pre-mature mdNase1L3 (position 75 without SP, Fig 1A) and was included in the previous study [37]. Mutation nt-914 was transferred into the present study during cloning the pPink α -HC expression vector and causes an exchange of Lys (K) to Arg(R)305 (position 280 without SP) in the second NLS, which is located in the basic C-terminal tail of mdNase1L3 (Fig 1A). The mutation is chemically conservative (basic) and outside the regions that are responsible for catalytic activity and DNA or actin binding. In addition, also human DNase1L3 shows phylogenetic changes between K and R in the basic C-terminus [37]. Thus, the K305R exchange is highly likely to be devoid of significance for the results obtained in the present study.

Transformation of electrocompetent *PichiaPinkTM pastoris*

For transformation, a glycerol stock of strain 4 of *PichiaPinkTM pastoris* (Invitrogen) was streaked on an YPD-plate (1% (w/v) yeast extract (Gibco-BRL), 2% (w/v) peptone (Foremedium), 2% (w/v) dextrose, 2.4% (w/v) agar (Carl Roth), and 50 μ g/ml ampicillin (Sigma-Aldrich) and grown for 3–5 days at 28°C. As a starter culture, 10 ml YPD in a 100 ml Erlenmeyer baffled flask were inoculated with a colony, cultured at 28°C and 250 rpm for 1–2 days to OD₆₀₀ 6. To generate electrocompetent cells, 100 ml YPD were inoculated to OD₆₀₀ 0.2 with the starter culture and grown for 1–2 days at 28°C and 250 rpm in a 1 l Erlenmeyer baffled flask to OD₆₀₀ 1.3–1.5. After each sedimentation step at 1,500g for 5 min at 4°C, the cells were washed twice in 250 and 50 ml of ice-cold water and thereafter resuspended in 10 and 0.3 ml of 1 M sorbitol, respectively.

For transformation 80 μ l of fresh electrocompetent cells in 1 M sorbitol were mixed with 10 μ g vector linearized with *Afl*III. The cells were transferred to an ice-cold 0.2 cm electroporation cuvette and electroporated at 1,500 V using the Electroporator 2510 (Eppendorf). After pulsing, 1 ml ice-cold YPDS (YPD with 1 M sorbitol) was added, the cells were mixed and incubated for 2 hours at 28°C without shaking. Aliquots of 200 μ l were spread on Pichia adenine drop-out plates (PAD: 100 mM potassium phosphate buffer (PPB), pH 6.0, 0.2% (w/v) Kaiser's SC-Ade mixture (Foremedium), 1.34% (w/v) yeast nitrogen base (YNB, Foremedium), 2% (w/v) dextrose, 2.4% (w/v) agar, and 50 μ g/ml ampicillin) and incubated at 28°C until white colonies were formed. Single colonies were re-streaked on fresh plates. Starter cultures of colonies were prepared in 10 ml Synthetic Complete Dextrose adenine drop-out medium (SCD-Ade: 100 mM PPB, pH 6.0, 0.2% (w/v) Kaiser's SC-Ade mixture, 2% (v/v) dextrose, 1.34% (w/v) YNB, 0.0004% (w/v) biotin (Sigma-Aldrich), and 50 μ g/ml ampicillin) in a 100 ml Erlenmeyer baffled flask and cultured at 28°C and routinely 250 rpm to OD₆₀₀ 6. For detection of transformed clones, 1 μ l of a 1:10 starter culture dilution was used in a PCR specific for the expression cassette of pPink α -HC (primers AOX1 and CYC1, Table 1). An aliquot of the PCR reaction was analyzed by 1.5% (w/v) Tris-borate/EDTA agarose gel electrophoresis with subsequent EtBr-staining. As a marker, the GeneRuler 1 kb DNA Ladder was used (ThermoFisher Scientific).

Expression of recombinant proteins

For biomass production of *P. pastoris*, 500 ml growth medium were inoculated with a starter culture to OD₆₀₀ 0.05 in a 5 l Erlenmeyer baffled flask. The growth culture was incubated overnight at 28–30°C under constant shaking at 250–300 rpm and grown to OD₆₀₀ 6. Either Synthetic Complete Glycerol adenine drop-out (SCG-Ade) medium (SCD-Ade with 1% (v/v) glycerol instead of dextrose) or Buffered Glycerol-complex Medium (BMGY: 100 mM PPB, pH 6.0, 1% (w/v) yeast extract, 2% (w/v) peptone, 1% (v/v) glycerol, 1.34% (w/v) YNB, 0.0004% (w/v) biotin, and 50 μ g/ml ampicillin) was used. After the growth culture, the cells were sedimented at 1,500 g, washed with 500 ml PBS, pH 6.0, for 30 min at RT, sedimented again, suspended in 50 ml expression medium to OD₆₀₀ 60, and transferred to a 500 ml Erlenmeyer non-baffled flask. Either Synthetic Complete Methanol adenine drop-out (SCM-Ade) medium (SCG-Ade with 0.5% (v/v) methanol and 100 mM MES-buffer, pH 6.0, instead of glycerol and PPB) or Peptone Methanol medium (PM: 100 mM MES-buffer, pH 6.0, 0.5% (w/v) peptone, 0.5% (v/v) methanol, 1.34% (w/v) YNB, 0.0004% (w/v) biotin, and 50 μ g/ml ampicillin) was used. The expression culture was incubated for 24 hours at 28–30°C under constant rotary shaking at 175 rpm. Subsequently, the cells were sedimented at 1,500 g and the cell-free SN was collected, filtrated through a 0.45 μ m filter unit (Millipore) and supplemented with 1 mM NaN₃.

Diethylaminoethyl-cellulose anion-exchange chromatography

For purification of recombinant protein from SN or dialysate, DEAE-cellulose anion-exchange chromatography was employed. The SN or the dialysate diluted 1:4 with chromatography (C)-buffer (25 mM MES, pH 6.0) was run with 1 ml/min through a glass column loaded with 2 ml of activated and equilibrated DE53-cellulose (Whatman Biosystems). Afterwards, the column was washed with 20 ml C-buffer and eluted with portions of 10 ml C-buffer containing increasing amounts of 50–500 mM NaCl. Subsequently, 2 mM CaCl₂ was added to the elution fractions to stabilize the 3D-structure of the DNases and to protect them against proteolysis [58, 59]. For maturation of pre-mature α MF-DNase1 prior to DEAE-cellulose chromatography, the SN was first dialyzed against 25 mM MES, pH 6.0, containing 2 mM CaCl₂, 2 mM

MgCl₂ and 1 mM NaN₃ using 30K filter units (Pierce) and incubated for 48 hours at 37°C. After DEAE-cellulose chromatography and prior to gel-filtration of rmDNase1, elution fraction E150 was concentrated with a 3K filter unit (Amicon). For purification of rmDNase1L2 and rmDNase1L3 by Heparin-Sepharose affinity chromatography, elution fraction E200 (rmDNase1L2) diluted 1:2 with Heparin-Sepharose C-buffer or the flow through (FT, rmDNase1L3) of the DEAE-cellulose chromatography was used.

Heparin-Sepharose affinity chromatography

For purification of recombinant protein by Heparin-Sepharose affinity chromatography, 1 ml of Heparin-Sepharose (GE Healthcare) was loaded in a glass column and equilibrated with 20 ml chromatography (C)-buffer (25 mM MES, pH 6.0, 100 mM NaCl, 2 mM CaCl₂, and 1 mM NaN₃). Diluted E200 (rmDNase1L2) or the FT (rmDNase1L3) of the DEAE-cellulose anion-exchange chromatography was run through the column followed by washing with 10 ml C-buffer. Elution occurred with 7.5 ml of C-buffer containing 1.5 M NaCl. The eluate was diluted 1:2 with C-buffer without NaCl and concentrated with a 3K filter unit for subsequent gel-filtration.

Gel-filtration

For gel-filtration, 80 ml swollen BioGel-P100 (Bio-Rad Laboratories) was loaded in a glass column and equilibrated with 2x storage buffer (50 mM MES, pH 6.0, 200 mM NaCl, 4 mM CaCl₂, and 2 mM NaN₃). Concentrated chromatography elution fractions were loaded on the gel bed and filtration was performed with 2x storage buffer. Fractions of 1 ml were collected and analyzed by SDS-PAGE and the hyperchromicity assay (HCA). Fractions containing mature nuclease were combined and concentrated to 2 mg/ml. The protein solution in 2x storage buffer was diluted 1:2 with glycerol and stored at -20°C. The storage buffer had been compiled based on different examples for commercially available DNase1 and was used to avoid extensive changes of the buffer compositions during the different steps of the purification procedure. Addition of proton donors to the storage or C-buffer was not tested, but does not seem to be recommended due to the two disulfide bridges in the native DNases of the DNase1 family.

SDS-polyacrylamide gel electrophoresis (SDS-PAGE)

For SDS-PAGE according to Laemmli [60], 4% (v/v) collecting and 10–12% (v/v) resolving gels were prepared. Routinely, 0.5 ml SN was concentrated 1:10 with a 3K filter unit, mixed with 4x SDS gel-loading buffer, heated to 95°C for 5 min (rmDNase1L2: 70°C for 10 min) and half of the sample was employed in SDS-PAGE. Corresponding amounts of the sample from different steps of the purification were prepared for SDS-PAGE. Electrophoresis was carried out at 80–120 V using Tris/glycine buffer (25 mM Tris, 192 mM glycine, 0.1% (w/v) SDS, pH 8.7). As a protein marker, PageRuler™ Prestained Protein Ladder (ThermoFisher Scientific) or Cozy Prestained Protein Ladder (highQu) was used. After electrophoresis, the gels were stained with 0.5% (w/v) Coomassie brilliant blue G-250 (Serva) dissolved in 40% (v/v) methanol and 10% (v/v) acetic acid. For destaining, the gel was incubated in 10% (v/v) ethanol and 5% (v/v) acetic acid. Gels were photographed and analyzed using the ChemiDoc™ XRS+ System with the ImageLab 5.0 software (Bio-Rad Laboratories).

Denaturing SDS-PAGE zymography (DPZ)

For DPZ, SDS-PAGE was performed with exception that the separating gels contained 100–200 µg/ml calf thymus DNA (Calbiochem). Samples, prepared as for SDS-PAGE, were diluted 1:20 to 1:200 in 1x SDS-sample buffer and 25 µl were loaded on the DPZ gel. For the detection

of the native DNases, murine tissue homogenates were prepared as previously described [37]. Electrophoresis, washing, nuclease reaction, and detection within the gel were performed as previously described [37].

Glycoprotein staining in SDS-polyacrylamide gels

Detection of glycoproteins by Periodic acid-Schiff staining in acrylamide gels was done according to Zacharius et al. [61]. In brief, gels were incubated in 12.5% (v/v) trichloroacetic acid for 30 min, rinsed in distilled water and immersed in 1% (v/v) periodic acid for 50 min. Having been washed in several batches of distilled water for 60 min, the gels were immersed in fuchsin-sulfite stain for 50 min in the dark. Subsequently the gels were washed first 3x 10 min in 0.5% (w/v) metabisulfite and secondly in distilled water over night. Destaining and storage were achieved by transferring the gels to 5% (v/v) acetic acid.

Hyperchromicity assay (HCA)

Specific activities of DNases were determined by HCA according to Kunitz [62]. The 1 ml reaction sample consisted of 50 µg/ml calf thymus DNA dissolved in 10 mM buffer, 0.1 mM CaCl₂ and either 1 mM MgCl₂, CoCl₂ or MnCl₂. The pH-values were adjusted using sodium acetate buffer for pH 5.0–5.5, MES-buffer for pH 6.0–6.5 and Tris-buffer for pH 7.0–9.0. Unless otherwise noted, we routinely used Tris-buffer, pH 7.0, containing 0.1 mM CaCl₂ and 1 mM MnCl₂ for measuring the specific activities of expression or purification samples. The absorbance at 260 nm was recorded for 1 min at RT in a quartz cuvette with 1 cm path length (Beckman DU640). One unit of nuclease is defined by an increase in absorbance of 0.001 per minute under the given conditions. For the calculation of equimolar amounts of the nucleases the molecular mass (MM) of the mature protein was used (Fig 1A). For actin inhibition the respective DNase and monomeric skeletal muscle α -actin were incubated in 50 µl of 10 mM buffer (as indicated in the figure captions) containing 0.1 mM CaCl₂ and 1% (v/v) protease inhibitor cocktail (PIC, Sigma-Aldrich) for 10 min on ice. Afterwards, the sample was completely employed in the HCA.

Lambda DNA digestion assay

Activity of DNases towards protein-free DNA was determined in an assay containing 25 µg/ml phage lambda DNA (ThermoScientific) dissolved in 10 mM buffer in the presence of 2 mM CaCl₂ and either 2 mM MgCl₂ or MnCl₂ for 30 min at 37°C. The pH-values were adjusted using sodium acetate buffer for pH 4.0–5.0, MES-buffer for pH 6.0 and Tris-buffer for pH 7.0–9.0. The reaction was stopped by addition of 10 mM EDTA and heating to 65°C for 5 min. An aliquot was analyzed by 1.5% (w/v) Tris-borate/EDTA agarose gel electrophoresis with subsequent EtBr-staining. In some experiments, the effect of 125 units/ml heparin (B. Braun Melsungen AG) on the DNase activities was investigated.

Chromatin digestion assay

Activity of DNases towards protein-complexed DNA (chromatin) was determined in a 200 µl reaction with 10⁵ nuclei of murine NIH-3T3 fibroblasts dissolved in 10 mM Tris-buffer, pH 7.5, 50 mM NaCl, 2 mM CaCl₂, 2 mM MgCl₂, and 1% (v/v) PIC. After incubation at 37°C for 18 hours, nuclear DNA was isolated with the QIAamp DNA Blood Mini Kit (Qiagen), and half of the DNA was analyzed by 1.5% (w/v) Tris-borate/EDTA agarose gel electrophoresis with subsequent EtBr-staining. In some experiments, the effect of 500 units/ml heparin on the DNase activities was investigated. Cell nuclei were isolated according to Stolzenberg et al. [63].

Actin polymerization assay

Actin polymerization was measured by following the increase in fluorescence intensity of 0.5 μ M pyrenyl-labeled monomeric skeletal muscle α -actin (pyrene-actin) added to 5 μ M non-labeled monomeric α -actin [64] over a period of 20 to 30 min after addition of 2 mM $MgCl_2$ using a Perkin-Elmer spectrofluorometer at excitation and emission wavelengths of 365 and 385 nm, respectively [65]. For the determination of the effect of the DNase variants on actin polymerization the respective DNase was pre-incubated for 10 min with equimolar monomeric α -actin at RT in reaction buffer (10 mM Hepes-buffer, pH 7.5, 0.1 mM $CaCl_2$ and 0.2 mM ATP) before the addition of 2 mM $MgCl_2$. Rabbit skeletal muscle α -actin was prepared from acetone powder as described [66].

Results

Establishment of rmDNase1L2 expression

Recombinant expression of the secretory murine DNases was carried out with the *Pichia-PinkTM pastoris* system using of α MF-SP [17]. We started with mDNase1L2, which as premature form consists of 278 amino acids (aa). After the cleavage of the N-terminal SP, mature mDNase1L2 consists of 257 aa with a calculated MM of ~29 kDa (Fig 1A and Table 2). For expression of rmDNase1L2, the cDNA encoding the mature nuclease was cloned in fusion to the α MF-SP (α MF-mDNase1L2) generating pPink α -HC/mDNase1L2. Strain 4 of

Table 2. Biochemical features of the secretory murine DNase1 family members.

Feature		mDNase1	mDNase1L2	mDNase1L3 [∞]
signal peptide *°		22 aa	21 aa	25 aa
mature protein *°		262 aa / 29.7 kDa	257 aa / 29.0 kDa	285 aa / 33.1 kDa
pI-value °		4.69	4.95	8.85
aa-sequence identity / similarity #	mDNase1	100%	53.4% / 70.2%	45.1% / 58.4%
	mDNase1L2	53.4% / 70.2%	100%	41.5% / 57.5%
	mDNase1L3 [∞]	45.1% / 58.4%	41.5% / 57.5%	100%
protein-free DNA-cleavage by HCA: pH-optimum specific activity [kU/nmol]	Ca^{2+} / Mg^{2+}	pH 7.5	pH 6.5	pH 8.0
		15.6±2.5	2.8±0.3	1.8±0.1
	Ca^{2+} / Co^{2+}	pH 7.0	pH 7.0	pH 7.0
		7.7±0.6	1.4±0.3	1.6±0.1
	Ca^{2+} / Mn^{2+}	pH 8.0	pH 7.5	pH 7.5
		13.9±0.6	5.0±0.3	5.5±0.9
glycosylation*		N-18 / N-106	-	-
monomeric α -actin interaction	HCA (Ca^{2+} / Mg^{2+})	~50% inhibition (equimolar)	-	-
chromatin cleavage		random	bi-modular	internucleosomal
heparin interaction		-	binding	binding
	HCA	-	inhibition	inhibition
	λ -DNA assay	-	inhibition	inhibition
	chromatin assay	activation	switch to random cleavage	inhibition

EMBOSS Needle program of the European Molecular Biology Laboratory.

* UniProt Knowledgebase (UniProtKB).

° ExPASy Compute pI/Mw tool from the Swiss Institute for Bioinformatics.

∞ K305R (position 280 without SP, Fig 1A).

<https://doi.org/10.1371/journal.pone.0253476.t002>

*PichiaPink*TM *pastoris*, which displays reduced proteolysis of secreted recombinant proteins (i.e. a lack of proteinase A, proteinase B and carboxypeptidase Y due to a double knockout of *pep4* and *prb1*) [17], was transformed and transgenic clones were isolated (Fig 2A). Before optimization, SCG-Ade growth medium was used for biomass production and SCM-Ade for transgene expression. Cultures were incubated at 28–30°C in a shaking incubator at 250–300 rpm (growth, baffled flasks) or 175 rpm (expression, non-baffled flasks). In order to reach optimal ventilation, the ratio of culture and flask volume was always 1:10. Expression SN was concentrated and analyzed by SDS-PAGE and/or DPZ.

Interestingly, the SDS-PAGE showed that the SN of transgenic clones contained a prominent protein of ~34 instead of 29 kDa as calculated for mature mDNase1L2 (Fig 2B). This implies either post-translational modification or an aberrant mobility of rmDNase1L2 in SDS-PAGE. Additionally, proteins of 17–34 kDa were detectable, which resembled a degradation pattern (Fig 2B). However, the addition of protease inhibitors during expression and sample preparation did not prevent the hypothesized degradation (S1 Fig). Instead, we found that rmDNase1L2 is vulnerable to heat dependent degradation in acidic loading buffer (Fig 2C) as described for other proteins [67, 68]. To prevent degradation, rmDNase1L2 samples were heated for 10 min at only 70°C. Since the expression level of mature rmDNase1L2 appeared low, we doubled the expression cassette in the vector and observed an increased expression in transformed clones (Fig 2D).

Next, we evaluated whether the MeOH-induced protein pattern entirely resulted from rmDNase1L2 expression and performed DPZ. As expected, wild-type (WT) *P. pastoris* did not secrete appreciable nucleases (Fig 2E). In contrast, all clones transformed displayed excessive nuclease activity in the SN after induction. Most of the activity appeared as a smear of high MM migrating above 48 kDa (lowest detectable band of the smear). On the other hand, the assigned mature rmDNase1L2 detectable in SDS-PAGE (Fig 2D) appeared again as a distinct band of ~34 kDa in DPZ (Fig 2E). This is consistent with a functional expression of rmDNase1L2 in *P. pastoris*. To evaluate a plausible post-translational modification, N-glycosylation was investigated. Notably, de-N-glycosylation by PNGaseF or EndoHf resulted in the disappearance of the high MM smear in DPZ and transformed it into a single nuclease band of ~41 kDa (Fig 2F). In contrast, the mature rmDNase1L2 of ~34 kDa was unaffected by this treatment as it is not N-glycosylated. After de-N-glycosylation, the difference in MM between both detectable nuclease bands was ~7 kDa, which fits to the MM of the de-N-glycosylated pro-peptide of α MF-SP (14 and 7 kDa with and without glycosylation, respectively [69], Fig 1B). In summary, ~50% of rmDNase1L2 expressed is pre-mature and still contains an extensively N-glycosylated pro-peptide (Fig 2E). Because processing of α MF-DNase1L2 occurs inefficiently, we replaced the α MF-SP in the expression cassette by the SP of native mDNase1L2. Unfortunately, expression failed pointing to a functional loss of this mammalian SP in *P. pastoris* (S2 Fig).

In a further attempt, we tried to overcome the inefficient pro-peptide cleavage by co-expressing KEX2. Therefore, chimeric expression vectors for α MF-DNase1L2 and either Golgi-located full-length or truncated soluble KEX2 lacking the transmembrane domain (KEX2- Δ TM613) were cloned [57]. Despite successful transformation (Fig 3A), we found signs of proteolysis of mature rmDNase1L2 instead of an increased expression level (Fig 3B and 3C).

Optimization of rmDNase1L2 expression

In general, we followed the instructions of the Invitrogen user manual for the *PichiaPink*TM *pastoris* system [17]. However, several factors are critical for recombinant protein expression in *P. pastoris* [17, 70]. Routinely, we started our experiments using SCG-Ade growth and SCM-Ade expression medium to maintain the selection pressure. Subsequently, parameters

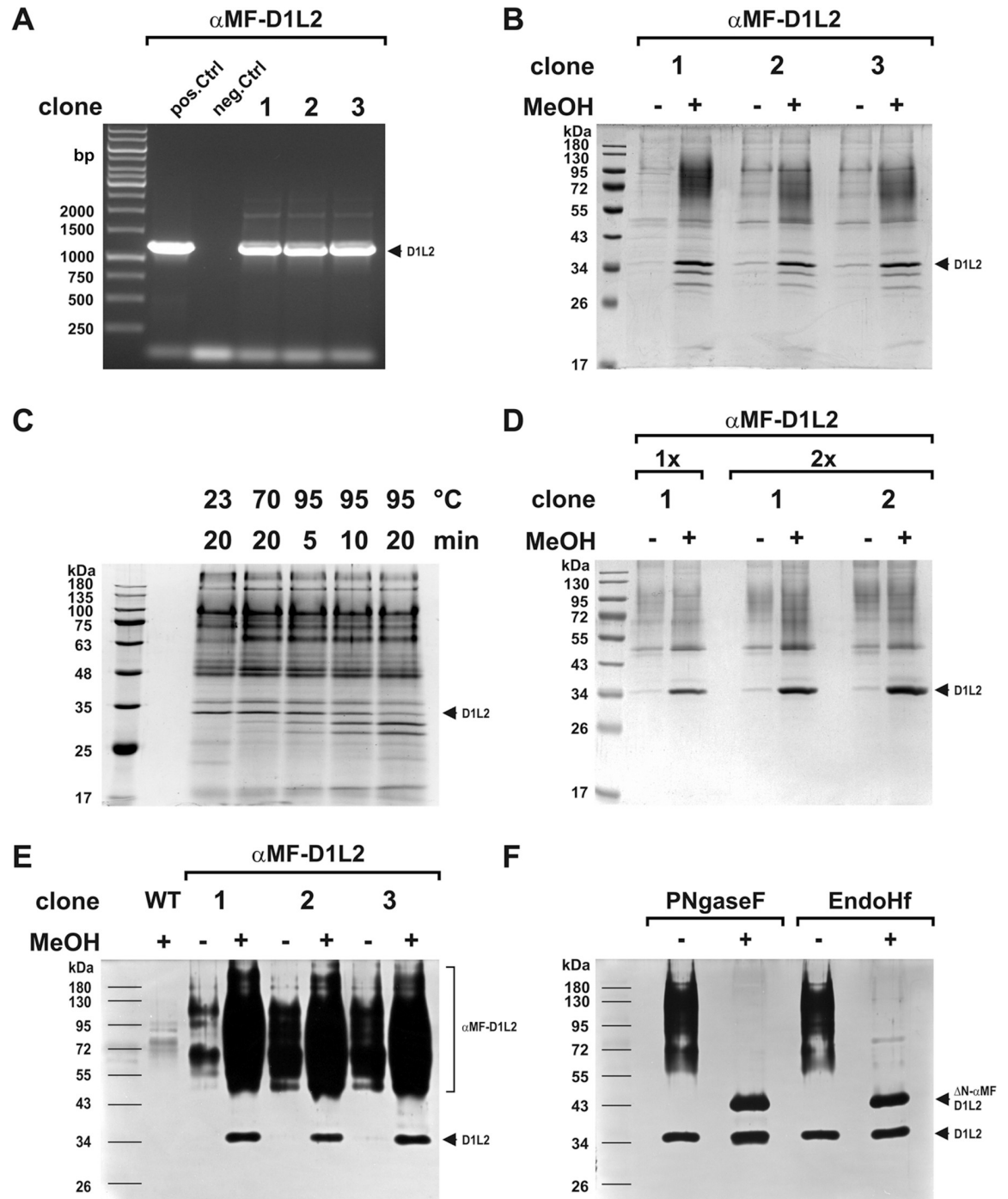


Fig 2. Establishment of rmdNase1L2 expression. (A) Detection of a single transgene integration for α MF-DNase1L2 (α MF-D1L2) in three transformed clones by expression cassette specific PCR (α MF-D1L2: 1197 bp, pos. Ctrl: vector, neg. Ctrl: water, marker: GeneRuler 1 kb DNA Ladder). (B) Detection of mature rmdNase1L2 (D1L2, ~34 kDa vs calculated 29 kDa) in the SN of MeOH-induced clones by SDS-PAGE and Coomassie staining. Note the heat-dependent instability of rmdNase1L2 in Laemmli sample buffer [60] as shown in (C). (D) Enhanced expression level of mature rmdNase1L2 by doubling the expression cassette for α MF-DNase1L2 in the transformed vector (1x vs 2x). (E) Functionality of rmdNase1L2 as verified by DPZ. Note the high MM nuclease smear with its lowest band at ~48 kDa representing pre-mature rmdNase1L2 that is still fused to the hyper-tri-N-mannosylated pro-peptide of α MF-SP (α MF-D1L2). (F) De-N-glycosylation (Δ N) by PNGaseF or EndoHf confers the high MM nuclease smear to a single Δ N- α MF-DNase1L2 nuclease band (~41 kDa) in DPZ (Δ N- α MF-D1L2: pre-mature rmdNase1L2 of ~34 kDa in fusion to the de-N-glycosylated 7 kDa pro-peptide of α MF-SP, Fig 1A and 1B). Marker: PageRuler™ Prestained Protein Ladder in (B, D, E, and F) and Cozy Prestained Protein Ladder in (C).

<https://doi.org/10.1371/journal.pone.0253476.g002>

were adapted to enhance expression as the following account shows: We found that washing cells with PBS prior to the induction of gene expression increased the expression level of rmDNase1L2 (Fig 4A). Since this increase might have been caused by a starvation effect, we varied the nutrient content during expression. However, changing the standard concentration of 0.2% (w/v) Kaiser's SC-Ade mixture in the SCM-Ade medium did not further increase protein expression (Fig 4B). Therefore, we tried to change the type of expression medium to reach this goal. Some investigators and the supplier propose Buffered Methanol-complex Medium (BMMY) with 1% (w/v) yeast extract and 2% (w/v) peptone (1x YP). Because BMMY contains high amounts of pigments, which are difficult to remove during purification, we reduced their content by omitting yeast extract and varying the amount of peptone (Peptone Methanol (PM) medium). At a concentration of 0.5% (w/v) peptone, PM was found to be even more efficient than the SCM-Ade expression medium (Fig 4B and 4C) and was therefore applied in all further experiments. Notably, no additional increase of expression was achieved using BMGY instead of SCG-Ade growth medium in combination with PM (Fig 4D). Instead, we observed that processing of pre-mature α MF-DNase1L2 (~48 kDa) to mature rmDNase1L2 (~34 kDa) depended on the amount of YP in the BMGY growth medium. Lowering its concentration to 0.125x was shown to be equivalent to SCG-Ade (Fig 4D). Further factors for an optimal production of mature rmDNase1L2 were a slightly acidic pH-value in the expression medium (pH 6.0) as well as an incubation temperature around 28°C (Fig 4E and 4F). The more alkaline the pH-value the more degradation of rmDNase1L2 occurred (Fig 4E). For growth, we routinely used potassium phosphate buffer, pH 6.0, whereas for expression MES, pH 6.0, was preferred, since phosphate might interfere with the nuclease activities. Phosphate or MES-buffer behaved equivalently in the expression experiments (compare Fig 4E with Fig 5A). Notably, an increased incubation time had no further promoting effect on expression (Fig 4F).

In summary, for optimal expression we grew *P. pastoris* transgenic for *mDnase1l2* at 28°C and 250–300 rpm to OD₆₀₀ 6 using standard SCG-Ade medium, pH 6.0, washed the cells with PBS, pH 6.0, for 30 min at RT and finally performed expression with PM medium, pH 6.0, containing 0.5% (w/v) peptone at a culture density of OD₆₀₀ 60 at 28°C and 175 rpm for 24 hours.

Purification of rmDNase1L2 from culture supernatant

Mature mDNase1L2 has a pI-value of 4.95 with a charge of -8.2 at pH 6.0 (Table 2). Therefore, we chose DEAE-cellulose anion-exchange chromatography for its concentration from the cell-free SN of the expression cultures. For all preparation steps, the buffer of the expression medium (MES, pH 6.0) was maintained to avoid destabilization of rmDNase1L2. After dilution, the SN was loaded onto an equilibrated DEAE column. Performing SDS-PAGE and HCA, we found that rmDNase1L2 bound completely to the resin (Fig 5A). Stepwise elution was performed with buffer containing increasing concentrations of 50–500 mM NaCl. The major part of mature rmDNase1L2 eluted at 200 mM (E200), whereas most of pre-mature α MF-DNase1L2 and further proteins of high MM eluted at 150 mM NaCl (Fig 5A). Since elution fraction E200 still included contaminants of high MM (Fig 5A), we tested further purification methods and found that rmDNase1L2 of diluted E200 bound completely to equilibrated Heparin-Sepharose comparable to rmDNase1L3 [37] (Fig 5B). The FT contained the high MM contaminants and almost no nuclease activity. Elution occurred at 1.5 M NaCl with an efficiency of ~62%. However, E1500 still contained nuclease activity of high MM (\geq 48 kDa) representing pre-mature α MF-DNase1L2 (Fig 5C).

In order to achieve final purification we concentrated diluted E1500, performed gel-filtration and observed two elution peaks. The fractions of the second peak were concentrated, diluted by addition of glycerol and an aliquot was tested by DPZ. It contained pure mature

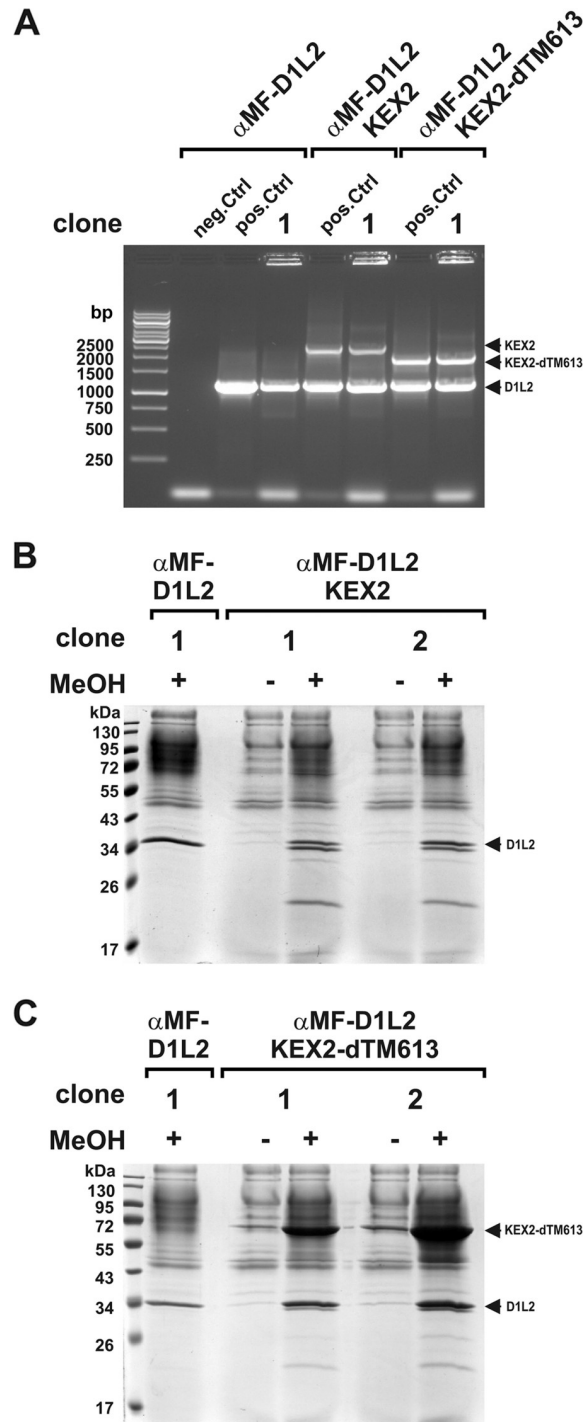


Fig 3. Co-expression of α MF-DNase1L2 with KEX2 or soluble KEX2- Δ TM613. (A) Detection of the different transgene integrations in transformed clones by expression cassette specific PCR (α MF-D1L2: 1197 bp, KEX2: 2597 bp, KEX2- Δ TM613: 2034 bp, pos.Ctrl: vector, neg.Ctrl: water, marker: GeneRuler 1 kb DNA Ladder). (B) Detection of rmDNase1L2 (D1L2) in the SN of MeOH-induced clones by SDS-PAGE and Coomassie staining reveals rmDNase1L2 degradation in clones co-expressing Golgi-located full-length KEX2. (C) Degradation of rmDNase1L2 also occurs in the presence of soluble truncated KEX2- Δ TM613. Marker in (B, C): PageRuler™ Prestained Protein Ladder.

<https://doi.org/10.1371/journal.pone.0253476.g003>

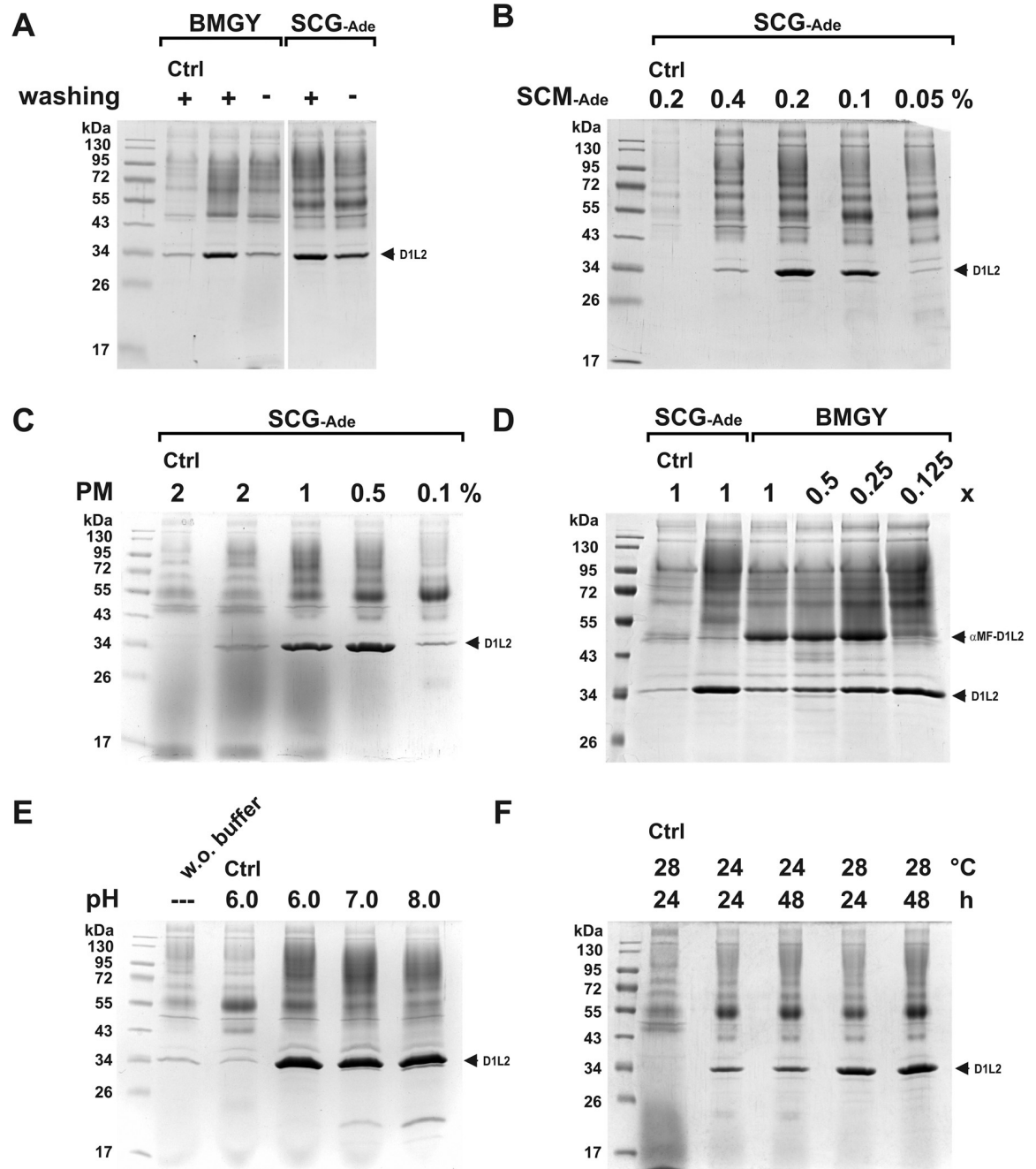


Fig 4. Optimization of rmDNase1L2 expression. (A) Washing cells with PBS, pH 6.0, between growth and expression (MeOH containing SCM-Ade medium) increased the expression of rmDNase1L2 (D1L2) independently of the growth medium (BMGY or SCG-Ade). (B) Dependence of rmDNase1L2 expression on the concentration of Kaiser's synthetic complete adenine drop-out mixture in the SCM-Ade expression medium. SCG-Ade growth medium was used. (C) Replacement of SCM-Ade by peptone methanol (PM) expression medium enhances the expression of rmDNase1L2 at an optimal concentration of 0.5% (w/v) peptone. (D) Dependence of the expression level and processing of pre-mature α MF-DNase1L2 (α MF-D1L2) to mature rmDNase1L2 on the nutrient content of the growth medium. Compared are 1x SCG-Ade (0.2% (w/v) Kaiser's SC-Ade) and BMGY medium (1x: 1% (w/v) yeast extract, 2% (w/v) peptone, YP) with varying YP-concentrations. (E, F) Expression of rmDNase1L2 using 1x SCG-Ade growth and PM-expression medium with 0.5% (w/v) peptone. (E) Stability of mature rmDNase1L2 depends on the pH-value of the expression medium (0.1 M potassium phosphate buffer). (F) Influence of the temperature and duration of the expression culture on the expression level of mature rmDNase1L2. In all experiments, the basal expression pattern of *P. pastoris* transgenic for *mDnase1L2* without MeOH induction was evaluated in parallel (Ctrl). Marker in (A-F): PageRuler™ Prestained Protein Ladder.

<https://doi.org/10.1371/journal.pone.0253476.g004>

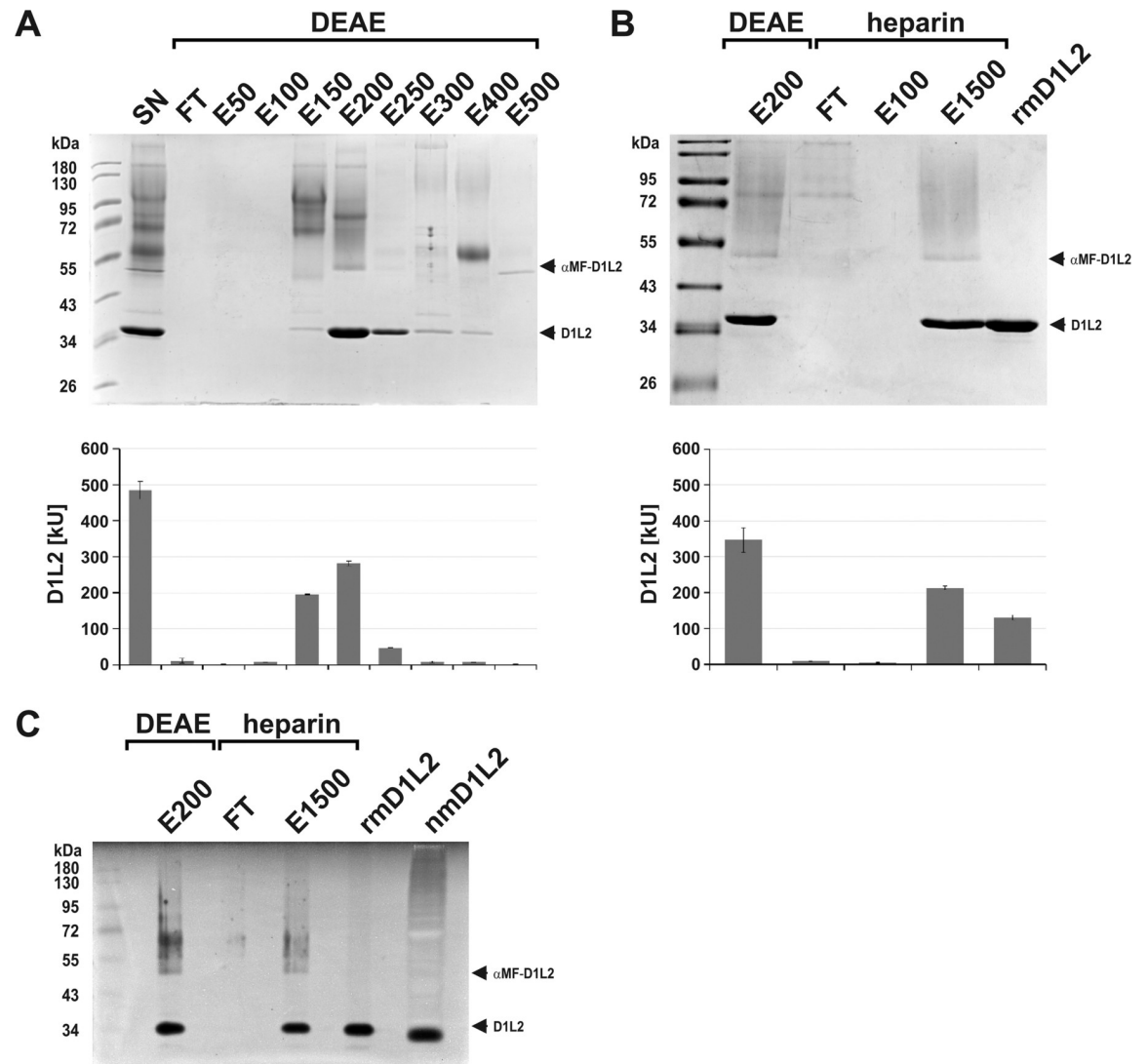


Fig 5. Purification of rmDNase1L2 from culture supernatant. (A) DEAE-cellulose anion-exchange chromatography of filtered and diluted SN. (FT: flow through, E50–500: elution fraction at 50–500 mM NaCl). (B) Purification of mature rmDNase1L2 (rmD1L2, D1L2) from DEAE elution fraction E200 by Heparin-Sepharose affinity chromatography. Final purification of mature rmDNase1L2 from E1500 was done by gel-filtration (last lane). (A, B) Top image: Coomassie-stained SDS-gel, lower image: absolute activity of the samples measured by HCA. (C) Successful separation of mature rmDNase1L2 from pre-mature α MF-DNase1L2 (α MF-D1L2) as shown by DPZ. The final pure rmDNase1L2 protein co-migrates with its native form (nmD1L2) present in a cutaneous tissue homogenate of a *Dnase1/Dnase1l3* double KO mouse (20 μ g protein loaded). Marker in (A–C): PageRuler™ Prestained Protein Ladder.

<https://doi.org/10.1371/journal.pone.0253476.g005>

rmDNase1L2 co-migrating with native mDNase1L2 present in a cutaneous tissue homogenate (Fig 5C). Purified rmDNase1L2 stored at -20°C was stable for at least one month as determined by HCA (4.96 ± 0.03 versus 4.12 ± 0.12 kU/nmol). About 26% of the nuclease activity present in the SN was isolated as mature rmDNase1L2 with a yield of maximal 3 mg/l expression culture.

Establishment and optimization of rmDNase1 expression

Next, we applied the protocol for expression of rmDNase1L2 to mDNase1. Mature mDNase1 consists of 262 aa with a calculated MM of ~ 30 kDa excluding any N-linked glycosylation (Fig

1A and Table 2). For expression, the cDNA for mature mDNase1 cloned in fusion to α MF-SP in pPink α -HC was used to transform strain 4 of *PichiaPinkTM pastoris* and positive clones were selected. We started with SCG-Ade growth and PM expression medium and also left other parameters identical to those for rmDNase1L2. In contrast to rmDNase1L2, a single expression cassette sufficed to reach elevated rmDNase1 activity. However, only pre-mature α MF-DNase1 (~51 kDa) was detectable (Fig 6A). Since an impact of the growth medium on processing of pre-mature α MF-DNase1L2 existed (Fig 4D), we tested BMGY with reduced YP and found an optimized processing of pre-mature to mature rmDNase1 (~37 kDa) at a concentration of 0.015x. Regarding the rmDNase1 activity however, BMGY with a higher YP content was more effective (Fig 6A). Therefore, we chose BMGY with 0.25x YP in combination with PM expression medium for the next experiments. A further reason for this was found by chance: Incubation of SN for 24–48 hours at 37°C led to the trimming of the α MF-SP with conversion of premature to mature rmDNase1. This process depended on the prior dialysis of the SN and occurred without loss of function as proved by HCA (Fig 6B). Trimming was mediated by a protease(s) in the SN, since it was retarded by addition of the protease inhibitor AEBSF (Figs 6B and S3). The protease concentration depended on the growth conditions and was greatest at 30°C and during shaking at 300 rpm for maximal ventilation (S3 Fig). However, protease release occurred during expression, since cells were prior washed with PBS.

Purification of rmDNase1 from culture supernatant

Mature mDNase1 has a pI-value of 4.69 with a charge of -10.2 at pH 6.0 (Table 2). Thus, having trimmed the α MF-SP in the dialyzed SN, we performed DEAE-cellulose anion-exchange chromatography analogous to rmDNase1L2. Binding was complete and elution occurred at 150 mM NaCl with an efficiency of ~74% and high purity (Fig 6C). In order to remove minor contaminants (Fig 6C) we subsequently performed gel-filtration identical to rmDNase1L2. Fractions with pure mature rmDNase1 were concentrated and samples were analyzed by DPZ. Our results show that pre-mature α MF-DNase1 was transformed entirely into mature rmDNase1, which was subsequently purified to homogeneity. It co-migrated with native mDNase1 present in a murine lacrimal tissue homogenate (Fig 6D). Similar to native mDNase1 from the parotid gland and fibroblastic rmDNase1 [37], the rmDNase1 produced by *P. pastoris* possessed two N-glycosylations, which, in contrast to mDNase1 expressed by mammalian cells, were entirely of the high-mannose type (Fig 6E). Analogous to rmDNase1L2, rmDNase1 stored at -20°C was stable for at least one month as determined by HCA (5.09±0.11 versus 4.12±0.05 kU/nmol). About ~35% of the nuclease activity present in the SN was isolated as pure mature rmDNase1 with a maximal yield of 9 mg/l expression culture.

Establishment and optimization of rmDNase1L3 expression

Finally, we attempted the expression of mature mDNase1L3, which consists of 285 aa with a calculated MM of ~33 kDa (Fig 1A and Table 2). For expression, the cDNA encoding mature mDNase1L3 was cloned in fusion to the α MF-SP in pPink α -HC. Unintentionally the cDNA contained a nucleotide exchange, which led to a conservative K to R mutation in the second NLS (see Materials and methods). Comparable to the results for rmDNase1L2, two expression cassettes were necessary to reach elevated nuclease activity in the SN of transgenic clones (Fig 7A). Again, we optimized expression and found analogous to rmDNase1 that BMGY growth medium with 0.25x YP in combination with PM expression medium was optimal. Most of rmDNase1L3 in the SN was mature and migrated at ~35 kDa in SDS-PAGE, whereas pre-mature α MF-DNase1L3 migrated at ~49 kDa (Fig 7A).

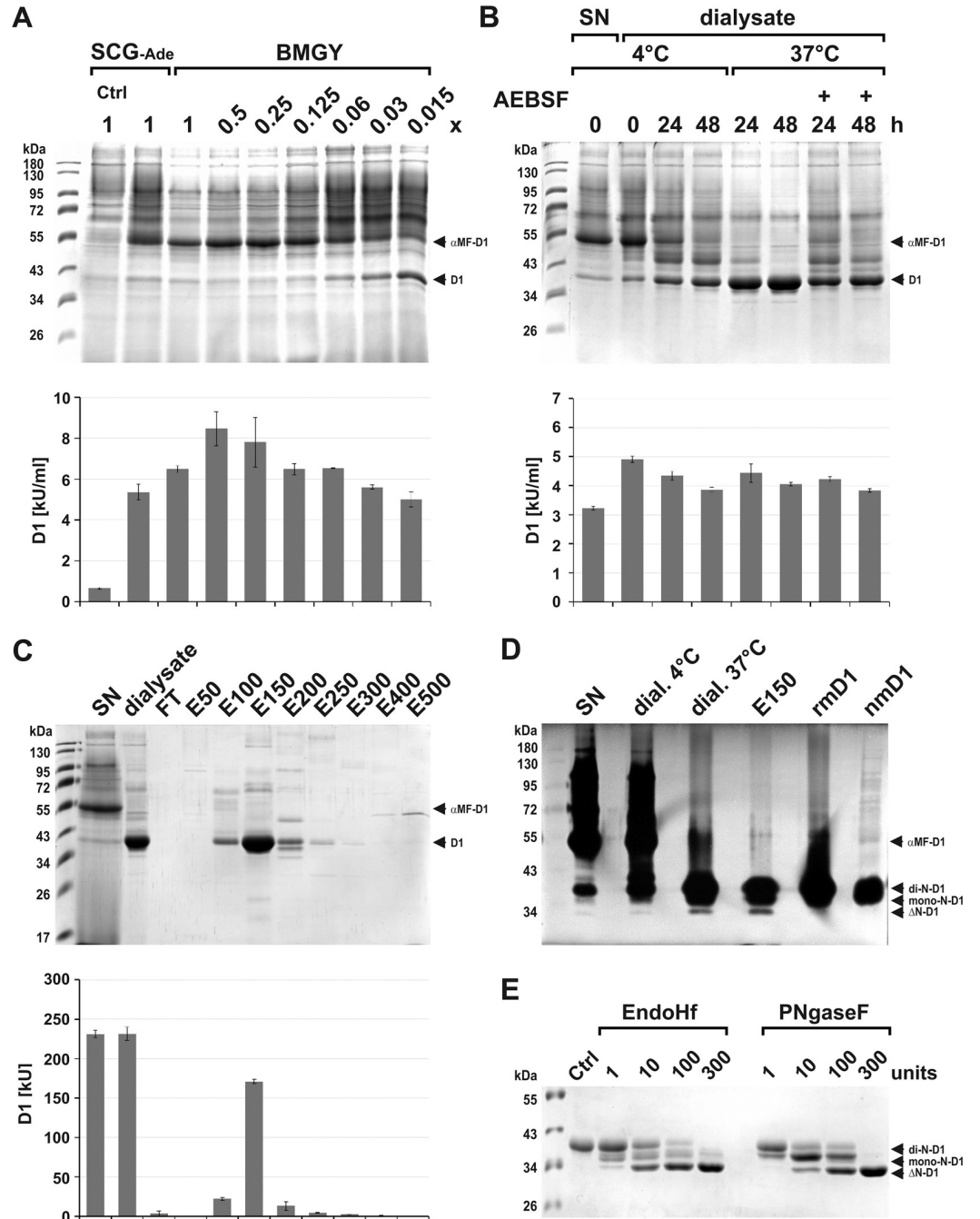


Fig 6. Establishment of expression and purification of rmdDNase1 from culture supernatant. (A) Expression and processing of pre-mature αMF-DNase1 (αMF-D1, ~51 kDa) to mature rmdDNase1 (D1, ~37 kDa) depends on the choice and nutrient content (1x BMGY: 1% yeast extract, 2% (w/v) peptone) of the growth medium (PM expression medium was used). (B) Temperature, time and protease dependent processing of pre-mature αMF-DNase1 to mature rmdDNase1 in dialyzed SN in the presence and absence of the protease inhibitor AEBSF. (C) Purification of mature rmdDNase1 from dialyzed and processed SN by DEAE-cellulose anion-exchange chromatography (FT: flow through, E50-500: elution fraction at 50–500 mM NaCl). (A-C) Top image: Coomassie-stained SDS-gel, lower image: specific activity of the samples measured by HCA. (D) Successful separation of mature rmdDNase1 from pre-mature αMF-DNase1 as shown by DPZ. Purified rmdDNase1 co-migrates with native mDNase1 (nmD1) present in a lacrimal tissue homogenate of a WT mouse (50 ng protein loaded). (E) Analysis of de-N-glycosylation by EndoHf and PNGaseF reveals di-N-glycosylation (mannosylation) of rmdDNase1 by DPZ. (rmdDNase1: di-N-glycosylated ~ 37 kDa, mono-N-glycosylated ~35 kDa and ΔN-glycosylated ~ 33 kDa). Marker: PageRuler™ Prestained Protein Ladder.

<https://doi.org/10.1371/journal.pone.0253476.g006>

Purification of rmDNase1L3 from culture supernatant

Mature mDNase1L3 has a pI-value of 8.85 with a charge of +9.91 at pH 6.0 (Table 2). Although rmDNase1L3 did not efficiently bind to DEAE-cellulose at pH 6.0, we applied it to remove contaminants. Therefore, the diluted SN was loaded on an equilibrated DEAE-cellulose column. About 55% of rmDNase1L3 activity remained in the FT, whereas contaminants bound and eluted at 0.5 M NaCl (Fig 7B). The FT was further processed by Heparin-Sepharose affinity chromatography. Similar to rmDNase1L2, rmDNase1L3 eluted at 1.5 M NaCl with a yield of ~74% (Fig 7B). However, E1500 still contained residual pre-mature α MF-DNase1L3 (Fig 7B). Final purification was achieved by gel-filtration comparable to rmDNase1 and rmDNase1L2. SDS-PAGE and DPZ showed that rmDNase1L3 was separated from pre-mature α MF-DNase1L3 and contaminants (Fig 7B and 7C). It co-migrated with native mDNase1L3 present in splenic tissue homogenate from a *Dnase1* KO mouse. Like rmDNase1 and rmDNase1L2, rmDNase1L3 stored at -20°C was stable for at least one month as determined by HCA (3.90 ± 0.56 versus 3.68 ± 0.16 kU/nmol). About ~10% of the nuclease activity present in the SN was isolated as pure mature rmDNase1L3 with a yield of maximal 3 mg/l expression culture.

Glycosylation of the rmDNases

Comparing the rmDNases by SDS-PAGE, we confirmed their purification to homogeneity in the mature form (Fig 7D). Since the MM of all nucleases appeared marginally higher in SDS-PAGE (rmDNase1: ~37 kDa, rmDNase1L2: ~34 kDa, and rmDNase1L3: ~35 kDa) than calculated (Fig 1A and Table 2), we stained the gel according to the Periodic acid-Schiff procedure to screen for glycosylation. In accordance with the de-N-glycosylation of rmDNase1 shown in Fig 6E, rmDNase1 is the only member of the secretory DNase1 family, which possesses glycosylation at all (Fig 7E).

Specific activities of the rmDNases

So far, the specific activities of the mDNase1 family members were not determined in comparison. A prerequisite for this is their comparable recombinant expression and purification with sufficient yields of pure protein, since it had not been possible to isolate all DNases to homogeneity from their natural sources. The most common assay allowing quantification is the HCA [62], which we applied at different pH-values in the presence of Ca^{2+} in combination with either Mg^{2+} ions or one of the essential trace elements Co^{2+} and Mn^{2+} as co-factors.

In the presence of Ca^{2+} and Mg^{2+} ions, the nucleases covered the broadest pH-range with respect to their optima (Fig 8A). Whereas rmDNase1L2 (2.8 ± 0.3 kU/nmol) displayed a slightly acidic optimum at pH 6.5, rmDNase1 (15.6 ± 2.5 kU/nmol) and rmDNase1L3 (1.8 ± 0.1 kU/nmol) showed a slightly basic optimum at pH 7.5 and 8.0, respectively (Fig 8A and Table 2). The difference in the specific activity between rmDNase1 and the others was greatest, i.e. ten times higher, at pH 7.5 (Fig 8A). Replacing Mg^{2+} by Co^{2+} ions led to an alignment of all optima to pH 7.0 with a difference of about five times between the specific activity of rmDNase1 and the others (Fig 8B and Table 2). The specific activity of rmDNase1L3 did not change significantly, whereas it was reduced by ~50% for rmDNase1 and rmDNase1L2 at optimal pH 7.0. Replacing Co^{2+} or Mg^{2+} by Mn^{2+} ions selectively increased the specific activities of rmDNase1L2 and rmDNase1L3 over a broad pH-range (Fig 8C and Table 2). Consequently, the specific activities of all nucleases aligned at neutral pH 7.0. At pH 7.5, rmDNase1 (10.4 ± 0.3 kU/nmol) was only twice more active than rmDNase1L2 (5.0 ± 0.3 kU/nmol) and rmDNase1L3 (5.5 ± 0.9 kU/nmol) (Fig 8C).

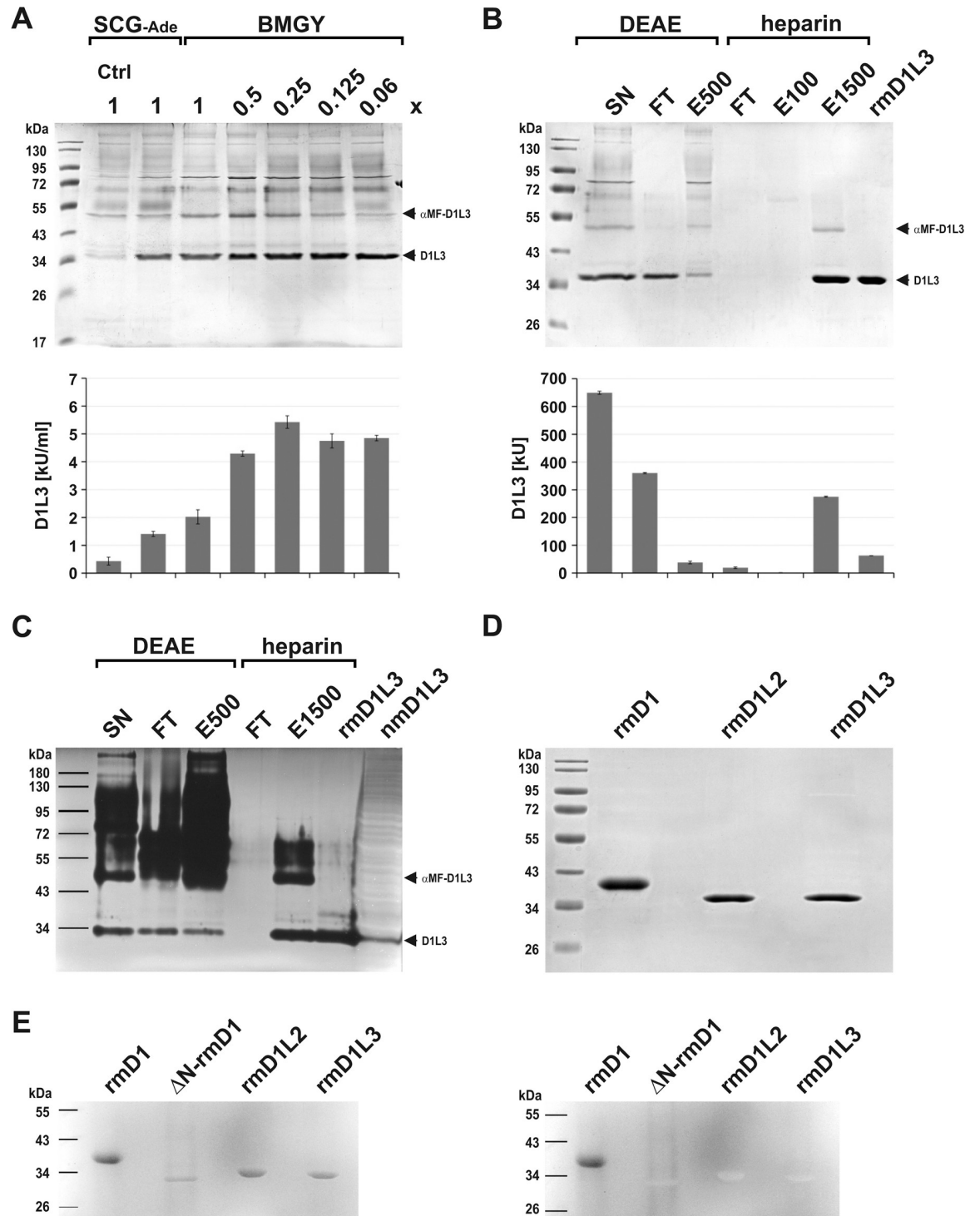


Fig 7. Establishment of expression and purification of rmdNase1L3 from culture supernatant. (A) Expression and processing of pre-mature αMF-DNase1L3 (αMF-D1L3, ~49 kDa) to mature rmdNase1L3 (D1L3, ~35 kDa) is less dependent on the choice and nutrient content of the growth medium (1x BMGY: 1% yeast extract, 2% (w/v) peptone) than that of rmdNase1 and rmdNase1L2 (PM expression medium was used). (B) Purification of mature rmdNase1L3 from diluted SN by DEAE-cellulose anion-exchange and Heparin-Sepharose affinity chromatography (FT: flow through, E50-1500: elution fraction at 50–1500 mM NaCl). (A, B) Top image: Coomassie-stained SDS-gel, lower image: specific nuclease activity of the samples measured by HCA. (C) Successful separation of pre-mature αMF-DNase1L3 from mature rmdNase1L3 as shown by DPZ. The final pure rmdNase1L3 protein co-migrates with native mDNase1L3 (nmD1L3) present in splenic tissue homogenate of a *Dnase1* KO mouse (40 μg protein loaded). (D) Direct comparison of

the purified recombinant secretory DNase1 proteins by SDS-PAGE and Coomassie-staining (each 4 μg). (E) Detection of glycosylation by Periodic acid-Schiff staining of an SDS-PAGE gel. Only rmDNase1 (rmD1) is glycosylated whereas de-N-glycosylated rmDNase1 (ΔN -rmD1), rmDNase1L2 (rmD1L2) and rmDNase1L3 (rmD1L3) lack glycosylation. Left image: stained gel prior to washing, right image: stained gel after washing with diluted acetic acid. Marker: PageRuler™ Prestained Protein Ladder.

<https://doi.org/10.1371/journal.pone.0253476.g007>

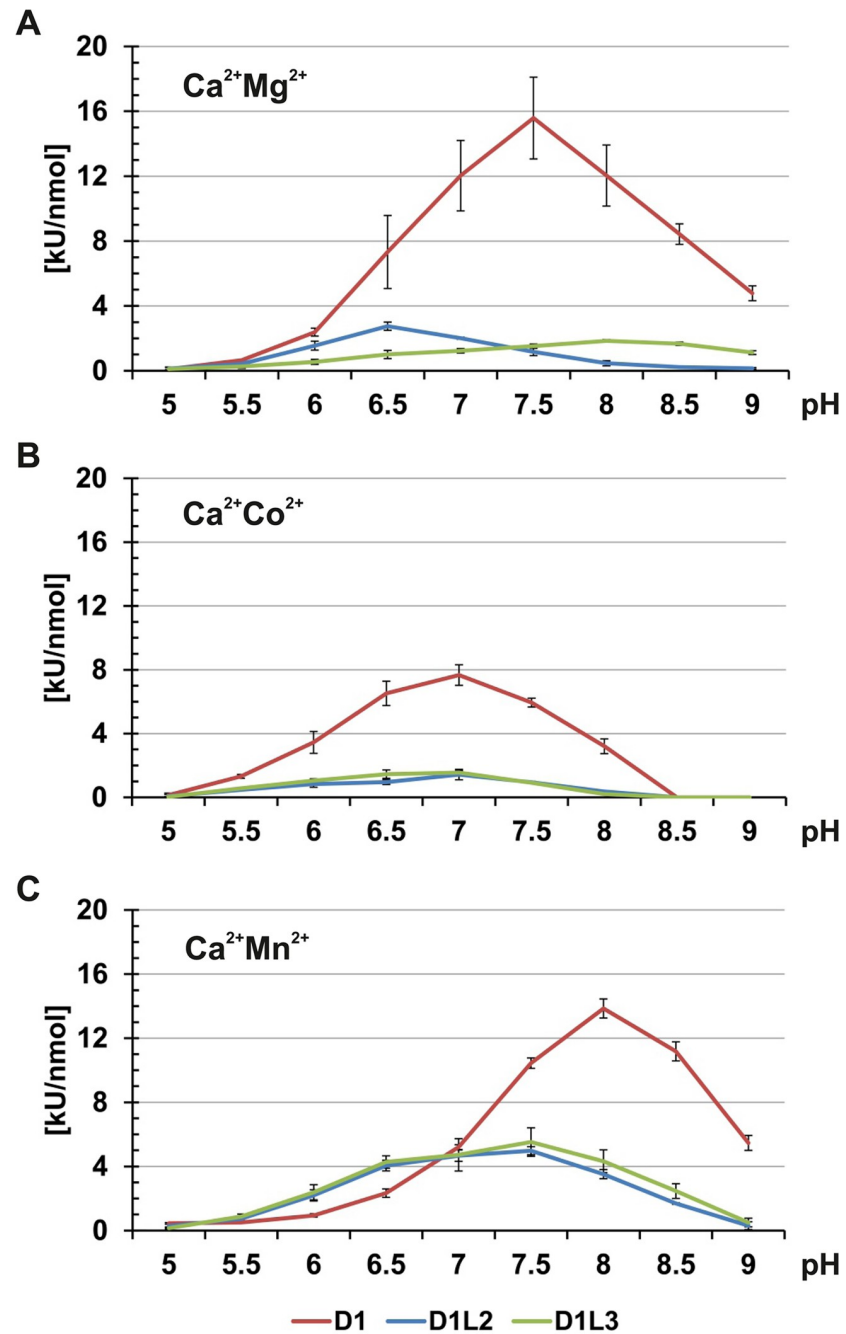


Fig 8. Specific activities of the rmDNases. Hyperchromicity assay at different pH-values in the presence of 0.1 mM CaCl₂ and either 1 mM MgCl₂ (A), CoCl₂ (B) or MnCl₂ (C). Equimolar amounts of the recombinant nucleases were tested (30 μM).

<https://doi.org/10.1371/journal.pone.0253476.g008>

Substrate specificities of the rmDNases

We confirmed the quantitative results obtained by HCA with a semi-quantitative assay investigating DNA degradation by agarose gel electrophoresis. Instead of plasmid DNA [37, 71], we used phage lambda DNA, which is linear and of defined length (48.5 kbp). In contrast to plasmid DNA, it has the advantage that degradation is directly visible by the generation of DNA fragments, whereas plasmid DNA first undergoes conformational changes from supercoiled, to relaxed and linear during DNA hydrolysis, which complicates a qualitative comparison of the DNase activities. Equimolar amounts of the nucleases were tested at different pH-values in the presence of Ca^{2+} with either Mg^{2+} or Mn^{2+} ions as a cofactor (Fig 9A). At pH 7.0 and in the presence of Mn^{2+} ions, all DNases exerted the same efficiency to degrade protein-free DNA, whereas at pH-values between 7.0 and 8.0 and in the presence of Mg^{2+} ions the greatest difference existed (Fig 9A). In agreement to previous studies [37], heparin inhibited rmDNase1L3 but not rmDNase1, and for the first time we demonstrate that rmDNase1L2 was also inhibited by heparin (Fig 9B). To evaluate whether these findings also apply to protein-complexed DNA, we performed a nuclear chromatin digestion assay (Fig 9C). In contrast to protein-free DNA, equimolar amounts of the DNases comparably degraded chromatin at pH 7.5 in the presence of Ca^{2+} and Mg^{2+} ions. Remarkably, rmDNase1 cleaved randomly, whereas rmDNase1L3 cleaved preferentially at internucleosomal sites [37] (Fig 9C). Notably, the cleavage ability of rmDNase1L2 appeared to be an intermediate, i.e. is bi-modular. Chromatin cleavage by rmDNase1 was enhanced by heparin, whereas rmDNase1L3 was inhibited [37]. In contrast to protein-free DNA, heparin did not inhibit rmDNase1L2 in chromatin cleavage but changed its cleavage pattern from bi-modular to exclusively random (Fig 9C).

Interaction of monomeric α -actin with the rmDNases

Finally, we evaluated binding of the DNases to monomeric skeletal muscle α -actin, which is well known for bovine DNase1 [51]. We observed that recombinant human (rh)DNase1 and rmDNase1 comparably inhibited α -actin polymerization at equimolar ratio (Fig 10A) illustrating their equal actin binding ability (Fig 1A). In contrast to 53% for rmDNase1, 80% of rhDNase1 activity was inhibited by equimolar amounts of monomeric α -actin (Fig 10B). Increasing the α -actin:DNase1 ratio led to complete inhibition of rhDNase1, whereas inhibition of rmDNase1 was again less effective (Fig 10B). These data hint to an altered conformation of the actin binding-site or its position relative to the catalytic centre in both DNases. Consistent with the non-conserved binding region for monomeric α -actin (Fig 1A), we found no significant effect of rmDNase1L2 and rmDNase1L3 on α -actin polymerization and *vice versa* of α -actin on the activity of both nucleases (S4 Fig). In comparison to Mn^{2+} , inhibition of rhDNase1 and rmDNase1 by monomeric α -actin occurs with higher efficiency in the presence of Mg^{2+} ions (S4 Fig).

Discussion

The present study describes recombinant expression of the secretory mDNase1 family members using *P. pastoris*. The major goal was to produce sufficient amounts of purified nucleases using a eukaryotic system resembling most closely the natural expression conditions and omitting interventions such as purification tags, protease recognition sites for post-expressional processing or optimization of the KEX2 cleavage site. Nevertheless, we are aware of the heterologous protein expression system. Unfortunately, standard protocols led to limited expression levels and therefore had to be modified as described. Increasing the gene dosage was effective, which is consistent with the recommendation to select multi-copy transgenic yeast or to increase the number of expression cassettes in the transformed vector [70, 72]. The first

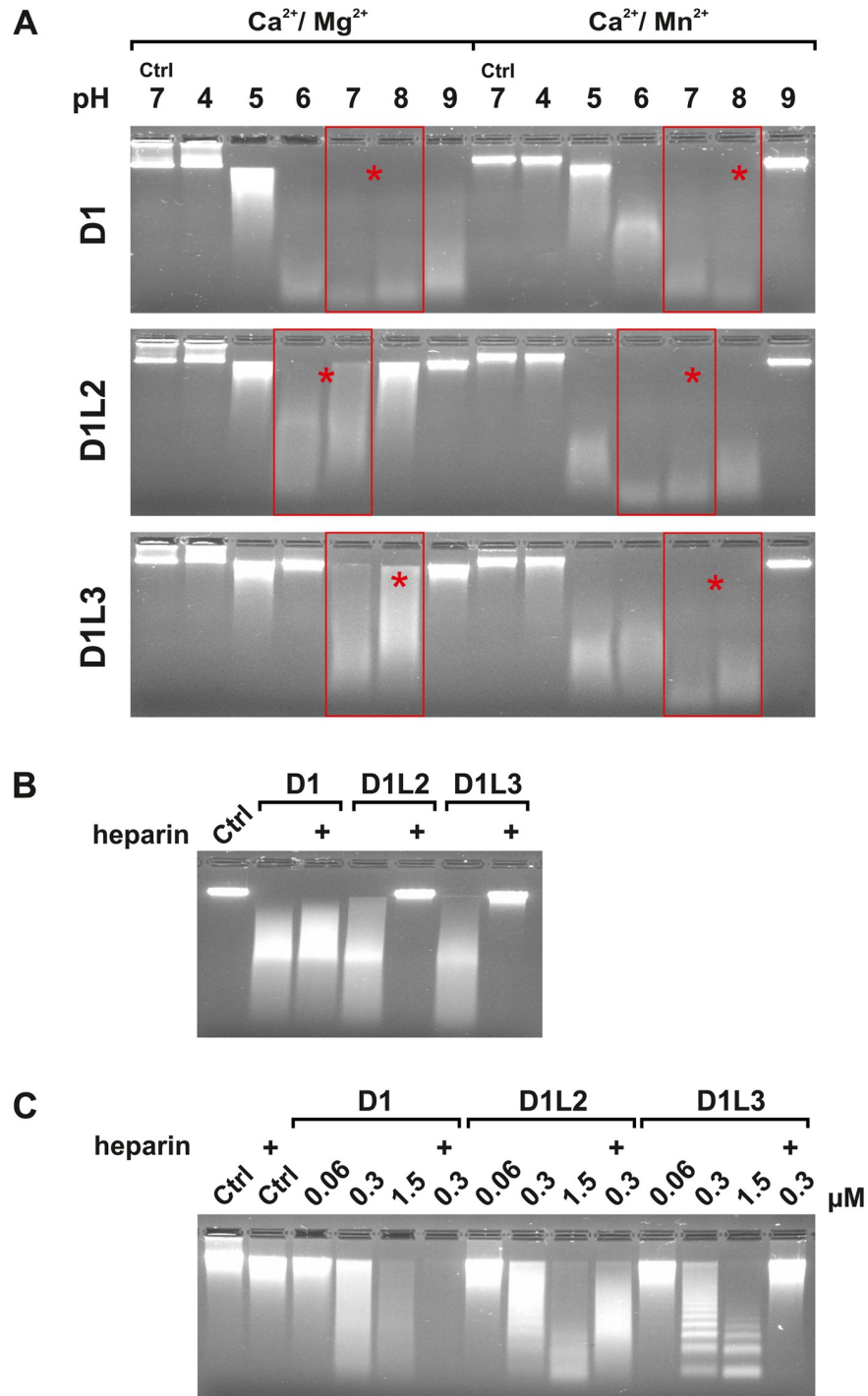


Fig 9. Substrate specific activities of the rmDNases. (A, B) Lambda DNA digestion at different pH-values in the presence of 2 mM CaCl₂ and either 2 mM MgCl₂ or 2 mM MnCl₂. Aliquots of the assay were analyzed by agarose gel electrophoresis and subsequent EtBr-staining. Equimolar amounts of the recombinant nucleases were tested (0.3 μM). Optimal pH-ranges are framed in red and the optimal pH-value estimated by HCA (Fig 8) is marked by an asterisk *. Consistent with the HCA, all three nucleases exert the same activity at pH 7.0 in the presence of Mn²⁺ ions, whereas at pH 7.5 in the presence of Mg²⁺ ions rmDNase1 (D1) exerts an activity, which is ten times higher as quantified by HCA. (B) In contrast to rmDNase1, heparin inhibits rmDNase1L2 (D1L2) and rmDNase1L3 (D1L3) in the protein-free lambda DNA assay at pH 7.0 in the presence of 2 mM CaCl₂ and 2 mM MnCl₂. (C) In contrast to protein-free lambda DNA in (A), all three nucleases exert an almost equal ability to degrade chromatin at pH 7.5 in the presence of 2 mM CaCl₂ and MgCl₂ using cell nuclei of murine NIH-3T3 fibroblasts. However, the cleavage mode differs (rmDNase1: random,

rmDNase1L2: bi-modular and rmDNase1L3: internucleosomal) as evaluated by agarose gel electrophoresis and subsequent EtBr-staining. Heparin accelerates the activity of rmDNase1 and inhibits that of rmDNase1L3 as previously shown [37]. In contrast to the lambda DNA assay, rmDNase1L2 is not inhibited by heparin but its cleavage mode changes from bi-modular to exclusively random.

<https://doi.org/10.1371/journal.pone.0253476.g009>

procedure, however, necessitates long-lasting high throughput screening, while the latter can be realized by a targeted and faster way. Besides gene dosage, optimizing protein maturation was found to be important since ~50% of the recombinant nucleases was pre-mature, i.e. was still bound to an extensively tri-N-glycosylated pro-peptide. Limited protein maturation and hyper-mannosylation are known for *P. pastoris* when using the α MF-SP. They result from an overload of the secretory machinery such as an inefficient pro-peptide cleavage by KEX2 [73, 74]. Known reasons are for example the size of the target protein or the removal of the di-basic spacer-peptide from the α MF-SP [75]. In addition, extensive glycosylation might sterically hinder binding of KEX2 to its substrate [76]. Appropriate methods to overcome the inefficient

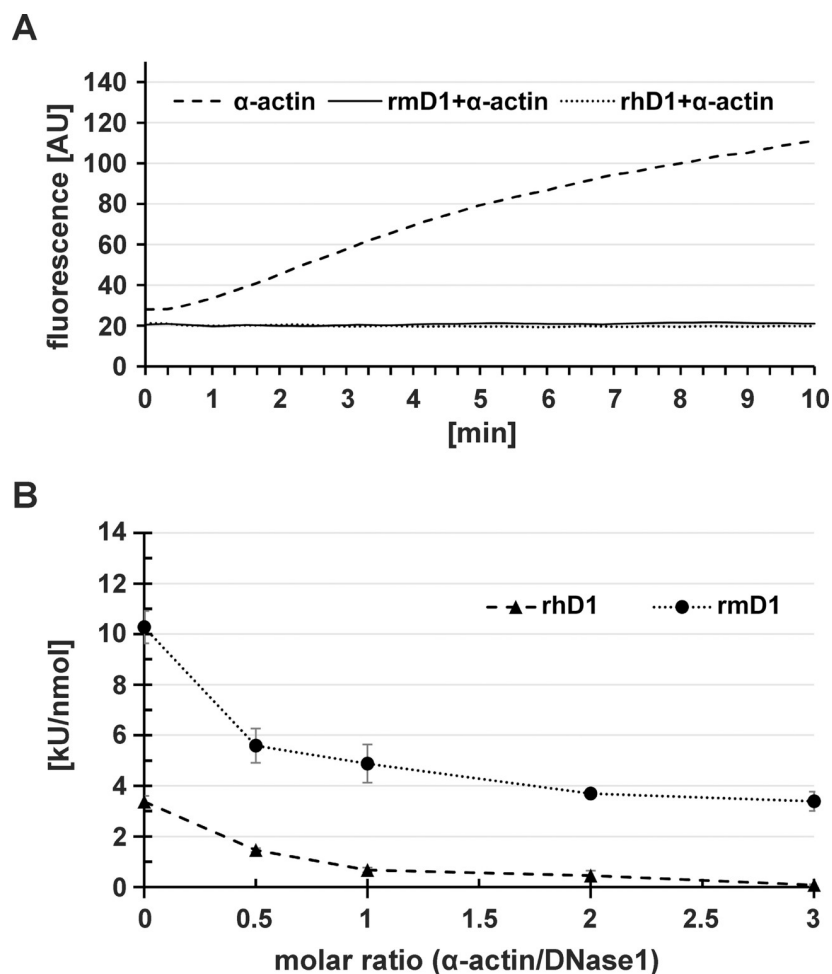


Fig 10. Interaction of monomeric α -actin with rhDNase1 and rmDNase1. (A) Polymerization of monomeric skeletal muscle α -actin supplemented with fluorescent pyrenyl-labeled monomeric α -actin to microfilaments in the absence and presence of rhDNase1 (rhD1, Pulmozyme™, Roche) or rmDNase1 (rmD1) at equimolar ratio (2.5 μ M). (B) Effect of increasing monomeric α -actin concentrations on the DNase1 activity as determined by HCA at pH 7.0 in the presence of 0.1 mM CaCl_2 and 1 mM MgCl_2 .

<https://doi.org/10.1371/journal.pone.0253476.g010>

maturation were reported to be the co-overexpression of KEX2 [77, 78], the post-expressional *in vitro* maturation by recombinant KEX2 [79] or the expression of the target protein with its native SP [70]. However, none of these approaches led to an improvement in our experiments.

Instead and consistent with previous findings, adjusting the equilibrium of recombinant protein translation and processing by starvation was successful [70, 80]. Thus, media with reduced nutrients and washing the cells with PBS prior to expression, improved protein expression and maturation. However, the latter finding could also be explained by a more efficient removal of glycerol, which is a repressor of the *AOX1* promoter [70, 81]. Appropriate media compositions appear to be very important and should be carefully evaluated for every protein of interest. Nutrient adaptation reduced glycosylation and increased maturation, which correlates with the theory that extensive glycosylation sterically interferes with KEX2 binding.

In addition to nutrient adaptation, we found a new procedure to process pre-mature rmDNase1 by N-terminal trimming employing dialysis of the SN. Maturation was facilitated by protease(s) in the SN and for their release *P. pastoris* had to be conditioned during biomass production. Trimming was not accompanied by loss of function and led to stable mature rmDNase1. We did not identify these protease(s), yet stress-induced up-regulation and release of yapsin 1 for example has been described [82]. However, yapsin 1 cannot be inhibited by AEBSF, which is in contrast to the retarded maturation of pre-mature DNase in the presence of AEBSF in our experiments [83]. Nevertheless, it cleaves the same di-basic motif as KEX2, pointing to the co-existence of comparable proteases in *P. pastoris* [84]. Furthermore, it has been shown that methanol, but not glycerol induces secretion of subtilisin 2, a PMSF inhibitable serine protease [85]. These examples demonstrate that although strain 4 of *PichiaPinkTM pastoris* lacks proteinase A, proteinase B and carboxypeptidase Y, other proteases might be released probably as a result of cell damage or due to misdirection under stress conditions [86].

After expression, purification procedures according to the biochemical properties of the nucleases were performed demonstrating that rmDNase1L2, as rmDNase1L3, binds to heparin [37]. After purification to homogeneity, all nucleases were shown to be functional and stable in storage buffer. The purified DNases were comparable to their mammalian originals even though the rmDNase1L3 contains an unintentional conservative K to R mutation in the second NLS (see Materials and methods). For example, rmDNase1, in contrast to the non-glycosylated rmDNase1L2 and rmDNase1L3, was found to be di-N-glycosylated as described in prior research [37]. This might explain its reduced processing by KEX2 (sterical hindrance) and its higher expression level probably caused by a greater proteolytic resistance [87]. We found no indication for the presence of protein or further contaminants influencing the biochemical characterization of the final DNase preparations. The prerequisite of contaminants would be that they have identical chromatographic behaviour and MM compared to the DNases. We assume that contaminations are rather unlikely or of only low amount, since it was possible to separate pre-mature from mature DNase differing by only 7 kDa by gel-filtration. It will be interesting to compare our DNase preparations with those using tags for affinity purification with respect to enzymatic properties and contaminants.

The subsequent biochemical analysis allowed a direct quantitative comparison of the specific activities of the mDNase1 members towards different substrates and under varying conditions for the first time. Previously, such studies were not possible because only defined volumes of expression SN or enriched preparations of His- or Myc-tagged nucleases were available for analysis [7, 37, 71]. Using HCA and the lambda DNA assay we showed that in the presence of the most abundant divalent cations Ca^{2+} and Mg^{2+} , the three DNases cover the broadest pH-range with respect to their optima. Under these conditions, mDNase1 is the major nuclease for the degradation of protein-free DNA with an optimum at neutral to slightly basic pH-value. This large activity difference in comparison to the other DNases diminishes in

the presence of either Co^{2+} or Mn^{2+} in combination with Ca^{2+} ions. While the presence of Co^{2+} ions equalizes the pH-optima of all DNases and reduces their activity, Mn^{2+} ions only equalize the pH-optima of rmDNase1L2 and rmDNase1L3 and increase their activity. However, they do not affect rmDNase1. Quite notably, at pH 7.0 in the presence of Mn^{2+} ions, all DNases exert an essentially identical activity. So far, the difference between the earth alkali (Ca^{2+} , Mg^{2+}) and the transition metal ions (Co^{2+} , Mn^{2+}), when used alone, is explained by the promotion of single versus double-stranded DNA hydrolysis [88]. However, this does not explain why Mn^{2+} , but not Co^{2+} , in comparison to Mg^{2+} ions enhances the activity of rmDNase1L2 and rmDNase1L3. It also does not explain why rmDNase1 is more active in the presence of Mg^{2+} than Mn^{2+} or Co^{2+} ions. Instead, it appears that the catalytic centre of mDNase1 is built differently from that of mDNase1L2 and mDNase1L3 and that all metal ions investigated have different abilities to coordinate the scissile phosphodiester bond of the DNA within the catalytic centre [14]. So far, no data are available about the 3D-structure of mDNase1L2 or mDNase1L3. In addition, no crystallographic data exist for mammalian DNases in the presence of cations other than Ca^{2+} and Mg^{2+} . It will be interesting to use the purified DNases for such investigations, as the necessary amounts can now be provided. Furthermore, it remains to be elucidated whether natural situations exist, under which the different cation-dependent DNA degrading activities might be of importance. Compared to the study of the human DNase1 family, which was expressed with His-tags, we determined similar pH-optima for the tag-free mDNases in the presence of Ca^{2+} and Mg^{2+} ions [7]. However, our study shows for the first time that the pH-optima vary with respect to the ion composition used. In addition to the estimation of pH-optima, specific activities were determined in our study for the first time. Previously determined pH-optima for rmDNase1 and rmDNase1L3 present within the SN of transfected culture cells differ from those in the present study [37]. This may be explained by the high bicarbonate and buffer concentration of the culture media, i.e. the SN, employed in small-scale plasmid DNA assays [37]. This finding points to the importance to use purified DNases for their biochemical characterization.

In contrast to the digestion of protein-free DNA, all nucleases display a comparable efficiency to degrade chromatin in the presence of Ca^{2+} and Mg^{2+} ions. This is consistent with the finding that mDNase1 and mDNase1L3 in the blood stream equally participate in the dissolution of NETs [41]. The chromatinolysis pattern differs from random (rmDNase1) to internucleosomal (rmDNase1L3) as previously described, although its biological consequence is unknown [71]. Thereby the pattern might depend on the charge and the tertiary structure of the nucleases. Non-glycosylated “small” basic proteins such as mDNase1L3 might more easily replace histone H1 from chromatin than the N-glycosylated acidic mDNase1. This scenario would preferentially render internucleosomal regions accessible for chromatinolysis by mDNase1L3, whereas mDNase1 might attack all exposed regions of the DNA backbone with a similar efficiency. Interestingly, rmDNase1L2 shows a bi-modular cleavage mode, which could be explained by the hypothesis described above: It possesses an acidic pI-value, but is not glycosylated and therefore, unlike mDNase1, might also gain access to internucleosomal regions. Displacement of histones from chromatin appears to be a necessary requirement for its optimal degradation. Heparin and proteases such as plasmin have this ability and thereby promote chromatinolysis by rmDNase1 as shown previously and in this study [37, 89]. Thus, the large difference in the specific activity between rmDNase1 and the other DNases towards protein-free DNA at pH 7.5 in the presence of Ca^{2+} and Mg^{2+} ions is maintained in the presence of heparin. Under these circumstances, the chromatin cleavage pattern of rmDNase1L2 switches from bi-modular to exclusively random, whereas the basic rmDNase1L3 is completely inhibited. The reason why rmDNase1L2 is not inhibited by heparin when cleaving chromatin instead of protein-free DNA might be explained by a higher affinity of the polyanionic heparin

to basic histones than to the acidic rmDNase1L2. Displacement of histones from chromatin ultimately results in the exclusively random DNA cleavage pattern by rmDNase1L2. From these results, it appears that heparin treatment should be carefully considered during therapeutic regimes. As long as DNase1 and DNase1L3 occur together in the presence of heparin, the enhanced chromatinolysis by DNase1 might compensate the inhibition of DNase1L3. However, in situations where macrophage derived DNase1L3 is probably dominating (inflammation), heparin treatment might be contra-indicated. In this context it remains to be elucidated, which natural role heparin has on DNase1L3. A common feature of rmDNase1L2 and rmDNase1L3 is their inability to bind to monomeric actin, which is again in agreement with their human counterparts [7]. This might point to their postulated role in intracellular chromatin cleavage of cells undergoing differentiation or apoptosis [21, 22, 48]. In contrast, DNase1 appears to function primarily extracellularly or in necrotic cells and is mostly inhibited by monomeric actin when released intracellularly [44, 45, 47, 52]. Alternatively or in parallel, residual amounts of liberated intracellular active DNase1 may induce the upregulation of apoptotic endonucleases as proposed recently [53]. Probably, heparin fulfills a role similar to monomeric actin by inhibiting misdirected DNase1L2 and DNase1L3.

Taken together, our results indicate that mDNase1L2 is an intermediate isoform of mDNase1 and mDNase1L3 with conserved features of both of them. Since mDNase1 and mDNase1L2 share the highest sequence identity and similarity and have both an almost equal identity and similarity to mDNase1L3, it appears that mDNase1L3 has diverged earlier from a common ancestor (Table 2). Whereas biochemical features present in all members of the DNase1 family can be definitely attributed to a common phylogenetic ancestor (see introduction), those shared by either mDNase1 or mDNase1L2 with mDNase1L3 might have been evolutionarily conserved. In contrast, individual features appear to be acquired during further differentiation. Thus, heparin binding, the ability for internucleosomal chromatin degradation and a preference for Ca^{2+} and Mn^{2+} ions appear to be characteristics of the common ancestor. In contrast, N-glycosylation (mDNase1), a preference for Mg^{2+} ions (mDNase1), monomeric actin binding (mDNase1), nuclear localization signals (mDNase1L3), or an exclusively random chromatin degradation (mDNase1) may have developed later individually. Thus, mDNase1L2 can be functionally regarded as an evolutionary intermediate isoform of mDNase1 and mDNase1L3.

Finally, our results demonstrate that the rmDNases are functional and suitable for further molecular and biological studies. In addition, it is worth considering their implementation as an additional therapeutic option for the treatment of micro-vessel congestion caused by aggregated NETs and damaged endothelial cells as found in patients suffering for instance from sepsis, autoimmune and cardiovascular diseases, and currently from a SARS-CoV2 infection [89, 90].

Conclusions

This manuscript demonstrates successful recombinant expression of the secretory (soluble) murine DNase1 family members in *P. pastoris* resulting in the purification of biologically functional DNases, which were shown to be comparable to their native counterparts. Limitations of expression such as a reduced α MF-SP pro-peptide processing with accumulation of premature DNase was overcome by adaption of the culture media compositions and by pro-peptide cleavage by stress-induced proteases. Our data describe for the first time an experimental protocol for the production and purification of these DNases in amounts suitable for investigation of their specific activities. Under the most prevalent extracellular conditions (high Ca^{2+} and Mg^{2+} ion concentrations, pH 7.4), rmDNase1, rmDNase1L2 and rmDNase1L3 display an equal ability to catalyse chromatinolysis, whereas rmDNase1 is significantly more active in

protein-free DNA degradation. This difference in activity changes when Mn^{2+} replace Mg^{2+} ions, since Mn^{2+} ions align the specific activities of the DNases. From the comparative characterization, it can be concluded that mDNase1L2, which was so far not extensively investigated, is an evolutionary intermediate isoform of the three DNases with respect to its biochemical properties.

Supporting information

S1 Fig. Protease inhibitors do not prevent degradation of rmDNase1L2. Analysis of SN prepared from expression cultures for rmDNase1L2 (SCM-Ade) by SDS-PAGE and Coomassie staining. (A) Expression in the absence or presence of the serine protease inhibitor AEBSF (1 mM) or bovine serum albumin (0.01% (w/v) BSA) to protect against a postulated protease degradation. (B) As described in Materials and methods, 0.5 ml SN was concentrated with a 3K filter unit by centrifugation. Addition of a protease inhibitor cocktail (PIC) during concentration and/or dialysis by H_2O did not prevent degradation of rmDNase1L2, which can be also seen in Fig 2B. Marker: PageRuler™ Prestained Protein Ladder in (A) and Cozy Prestained Protein Ladder in (B).

(TIF)

S2 Fig. Expression of rmDNase1L2 with its natural signal peptide. (A) Detection of single transgene integrations in a transformed clone for expression of mDNase1L2 with the α MF-SP (α MF-D1L2) in comparison to three clones for mDNase1L2 with its natural signal peptide (SP-D1L2) by expression cassette specific PCR (α MF-D1L2: 1197 bp, SP-D1L2: 1011 bp, pos. Ctrl: vector, neg. Ctrl: water, marker: GeneRuler 1 kb DNA Ladder). (B) Analysis of SN prepared from induced (MeOH) or not induced SCM-Ade expression cultures of the different clones by SDS-PAGE and Coomassie staining. Marker: PageRuler™ Prestained Protein Ladder.

(TIF)

S3 Fig. Protease release for α MF-DNase1 maturation depends on the grade of ventilation of the growth culture. Processing of pre-mature α MF-DNase1 (α MF-D1, ~51 kDa) in 2x dialyzed expression SN of *P. pastoris* grown in BMGY at 30°C and shaking at either 175 or 300 rpm in baffled flasks. Processing to mature rmDNase1 (D1, ~37 kDa) depends on protease(s) released into the PM expression medium in dependence of the ventilation of the growth culture. Optimal ventilation occurs at 300 rpm. The maturation can be retarded by the protease inhibitor AEBSF (1 mM) and occurs optimally in the presence of Ca^{2+} and Mg^{2+} ions at 37°C. Marker: PageRuler™ Prestained Protein Ladder.

(TIF)

S4 Fig. Interaction of monomeric α -actin with the rmDNase1 family members. (A) Polymerization of monomeric skeletal muscle α -actin supplemented with fluorescent pyrenyl-labeled monomeric α -actin to microfilaments in the absence and presence of rhDNase1 (rhD1, Pulmozyme™, Roche), rmDNase1 (rmD1), rmDNase1L2 (rmD1L2), or rmDNase1L3 (rmD1L3) at equimolar ratio (2.5 μ M). In contrast to rmDNase1 or rhDNase1, rmDNase1L2 and rmDNase1L3 did not influence α -actin polymerization, which indicates a lack of molecular interaction. (B) Upper bar chart: DNase activity in the absence (Ctrl) or presence of monomeric α -actin at optimal pH-value for all nucleases as determined by HCA with Tris-buffer, pH 7.0, in the presence of 0.1 mM $CaCl_2$ and 1 mM $MnCl_2$. Lower bar chart: HCA at optimal pH-value for the different nucleases in the presence of 0.1 mM $CaCl_2$ and 1 mM $MgCl_2$ using Tris-buffer, pH 7.5 (rhDNase1 and rmDNase1), Tris-buffer, pH 8.0 (rmDNase1L3) or MES-buffer, pH 6.5 (rmDNase1L2). The inhibition of rhDNase1 by binding to monomeric α -actin is stronger than of rmDNase1 and is enhanced in the presence of Mg^{2+} in comparison to Mn^{2+}

ions for both nucleases. In contrast to rmDNase1 or rhDNase1, no molecular interaction of rmDNase1L2 and rmDNase1L3 with monomeric α -actin could be detected. (TIF)

S1 Dataset.

(PDF)

S1 Raw images.

(PDF)

Acknowledgments

The authors appreciate the support provided by Prof. Dr. Beate Brand-Saberi and acknowledge the work of Katja Jakubowski on establishing mDNase1 expression in *P. pastoris* in the course of her master's thesis and cloning the *mDnase1l2* cDNA from skin during an internship. The vector pRS415/KEX2 was provided by Addgene, a global non-profit repository for plasmids and scientific education.

Author Contributions

Investigation: Lukas Verhülsdonk, Hans Georg Mannherz, Markus Napirei.

Methodology: Lukas Verhülsdonk, Markus Napirei.

Supervision: Markus Napirei.

Visualization: Markus Napirei.

Writing – original draft: Lukas Verhülsdonk, Markus Napirei.

Writing – review & editing: Hans Georg Mannherz.

References

1. Keyel PA. Dnases in health and disease. *Developmental biology*. 2017; 429(1):1–11. <https://doi.org/10.1016/j.ydbio.2017.06.028> PMID: 28666955.
2. McCarty M. Purification and properties of desoxyribonuclease isolated from beef pancreas. *J Gen Physiol*. 1946; 29:123–39.
3. Parrish JE, Ciccociola A, Wehert M, Cox GF, Chen E, Nelson DL. A muscle-specific DNase I-like gene in human Xq28. *Hum Mol Genet*. 1995; 4(9):1557–64. <https://doi.org/10.1093/hmg/4.9.1557> PMID: 8541839.
4. Rodriguez AM, Rodin D, Nomura H, Morton CC, Weremowicz S, Schneider MC. Identification, localization, and expression of two novel human genes similar to deoxyribonuclease I. *Genomics*. 1997; 42(3):507–13. <https://doi.org/10.1006/geno.1997.4748> PMID: 9205125.
5. Zeng Z, Parmelee D, Hyaw H, Coleman TA, Su K, Zhang J, et al. Cloning and characterization of a novel human DNase. *Biochem Biophys Res Commun*. 1997; 231(2):499–504. <https://doi.org/10.1006/bbrc.1996.5923> PMID: 9070308.
6. Shiokawa D, Tanuma S. Molecular cloning and expression of a cDNA encoding an apoptotic endonuclease DNase gamma. *Biochem J*. 1998; 332 (Pt 3):713–20. <https://doi.org/10.1042/bj3320713> PMID: 9620874; PubMed Central PMCID: PMC1219532.
7. Shiokawa D, Tanuma S. Characterization of human DNase I family endonucleases and activation of DNase gamma during apoptosis. *Biochemistry*. 2001; 40(1):143–52. <https://doi.org/10.1021/bi001041a> PMID: 11141064.
8. Oefner C, Suck D. Crystallographic refinement and structure of DNase I at 2 Å resolution. *J Mol Biol*. 1986; 192(3):605–32. [https://doi.org/10.1016/0022-2836\(86\)90280-9](https://doi.org/10.1016/0022-2836(86)90280-9) PMID: 3560229.
9. Gueroult M, Picot D, Abi-Ghanem J, Hartmann B, Baaden M. How cations can assist DNase I in DNA binding and hydrolysis. *PLoS computational biology*. 2010; 6(11):e1001000. <https://doi.org/10.1371/journal.pcbi.1001000> PMID: 21124947; PubMed Central PMCID: PMC2987838.

10. Nishikawa A, Mizuno S. The efficiency of N-linked glycosylation of bovine DNase I depends on the Asn-Xaa-Ser/Thr sequence and the tissue of origin. *Biochem J.* 2001; 355(Pt 1):245–8. <https://doi.org/10.1042/0264-6021:3550245> PMID: 11256970.
11. Pan CQ, Ulmer JS, Herzka A, Lazarus RA. Mutational analysis of human DNase I at the DNA binding interface: implications for DNA recognition, catalysis, and metal ion dependence. *Protein Sci.* 1998; 7(3):628–36. <https://doi.org/10.1002/pro.5560070312> PMID: 9541395.
12. Lahm A, Suck D. DNase I-induced DNA conformation. 2 A structure of a DNase I-octamer complex. *J Mol Biol.* 1991; 222(3):645–67. [https://doi.org/10.1016/0022-2836\(91\)90502-w](https://doi.org/10.1016/0022-2836(91)90502-w) PMID: 1748997.
13. Jones SJ, Worrall AF, Connolly BA. Site-directed mutagenesis of the catalytic residues of bovine pancreatic deoxyribonuclease I. *J Mol Biol.* 1996; 264(5):1154–63. <https://doi.org/10.1006/jmbi.1996.0703> PMID: 9000637.
14. Parsiegla G, Noguere C, Santell L, Lazarus RA, Bourne Y. The structure of human DNase I bound to magnesium and phosphate ions points to a catalytic mechanism common to members of the DNase I-like superfamily. *Biochemistry.* 2012; 51(51):10250–8. <https://doi.org/10.1021/bi300873f> PMID: 23215638.
15. Ulmer JS, Herzka A, Toy KJ, Baker DL, Dodge AH, Sinicropi D, et al. Engineering actin-resistant human DNase I for treatment of cystic fibrosis. *Proc Natl Acad Sci U S A.* 1996; 93(16):8225–9. <https://doi.org/10.1073/pnas.93.16.8225> PMID: 8710851.
16. Shiokawa D, Shika Y, Tanuma S. Identification of two functional nuclear localization signals in DNase gamma and their roles in its apoptotic DNase activity. *Biochem J.* 2003; 376(Pt 2):377–81. <https://doi.org/10.1042/BJ20030820> PMID: 12943533; PubMed Central PMCID: PMC1223774.
17. Invitrogen™-LifeTechnologies™. PichiaPink™ Expression System User Guide. https://assetsthermofishercom/TFS-Assets/LSG/manuals/pichiapink_expression_system_manpdf. 2014; MAN0000717.
18. Shiokawa D, Matsushita T, Shika Y, Shimizu M, Maeda M, Tanuma S. DNase X is a glycosylphosphatidylinositol-anchored membrane enzyme that provides a barrier to endocytosis-mediated transfer of a foreign gene. *J Biol Chem.* 2007; 282(23):17132–40. Epub 2007/04/06. <https://doi.org/10.1074/jbc.M610428200> PMID: 17416904.
19. Malferrari G, Mazza U, Tresoldi C, Rovida E, Nissim M, Mirabella M, et al. Molecular characterization of a novel endonuclease (Xib) and possible involvement in lysosomal glycogen storage disorders. *Exp Mol Pathol.* 1999; 66(2):123–30. <https://doi.org/10.1006/exmp.1999.2254> PMID: 10409440.
20. Los M, Neubuser D, Coy JF, Mozoluk M, Poustka A, Schulze-Osthoff K. Functional characterization of DNase X, a novel endonuclease expressed in muscle cells. *Biochemistry.* 2000; 39(25):7365–73. <https://doi.org/10.1021/bi000158w> PMID: 10858283.
21. Fischer H, Szabo S, Scherz J, Jaeger K, Rossiter H, Buchberger M, et al. Essential role of the keratinocyte-specific endonuclease DNase1L2 in the removal of nuclear DNA from hair and nails. *J Invest Dermatol.* 2011; 131(6):1208–15. <https://doi.org/10.1038/jid.2011.13> PMID: 21307874; PubMed Central PMCID: PMC3185332.
22. Fischer H, Buchberger M, Napirei M, Tschachler E, Eckhart L. Inactivation of DNase1L2 and DNase2 in keratinocytes suppresses DNA degradation during epidermal cornification and results in constitutive parakeratosis. *Scientific reports.* 2017; 7(1):6433. <https://doi.org/10.1038/s41598-017-06652-8> PMID: 28743926; PubMed Central PMCID: PMC5527052.
23. Lacks SA. Deoxyribonuclease I in mammalian tissues. Specificity of inhibition by actin. *J Biol Chem.* 1981; 256(6):2644–8. PMID: 6259139.
24. Napirei M, Ricken A, Eulitz D, Knoop H, Mannherz HG. Expression pattern of the deoxyribonuclease 1 gene: lessons from the Dnase1 knockout mouse. *Biochem J.* 2004; 380(Pt 3):929–37. <https://doi.org/10.1042/BJ20040046> PMID: 15015938; PubMed Central PMCID: PMC1224217.
25. Napirei M, Karsunky H, Zevnik B, Stephan H, Mannherz HG, Moroy T. Features of systemic lupus erythematosus in Dnase1-deficient mice. *Nat Genet.* 2000; 25(2):177–81. <https://doi.org/10.1038/76032> PMID: 10835632.
26. Martinez-Valle F, Balada E, Ordi-Ros J, Bujan-Rivas S, Sellas-Fernandez A, Vilardell-Tarres M. DNase 1 activity in patients with systemic lupus erythematosus: relationship with epidemiological, clinical, immunological and therapeutical features. *Lupus.* 2009; 18(5):418–23. <https://doi.org/10.1177/0961203308098189> PMID: 19318394.
27. Skiljevic D, Jeremic I, Nikolic M, Andrejevic S, Sefik-Bukilica M, Stojimirovic B, et al. Serum DNase I activity in systemic lupus erythematosus: correlation with immunoserological markers, the disease activity and organ involvement. *Clinical chemistry and laboratory medicine.* 2013; 51(5):1083–91. <https://doi.org/10.1515/cclm-2012-0521> PMID: 23183758.
28. Trofimenko AS, Gontar IP, Zborovsky AB, Paramonova OV. Anti-DNase I antibodies in systemic lupus erythematosus: diagnostic value and share in the enzyme inhibition. *Rheumatol Int.* 2016; 36(4):521–9. <https://doi.org/10.1007/s00296-016-3437-z> PMID: 26879320.

29. Fenton K, Fismen S, Hedberg A, Seredkina N, Fenton C, Mortensen ES, et al. Anti-dsDNA antibodies promote initiation, and acquired loss of renal Dnase1 promotes progression of lupus nephritis in autoimmune (NZBxNZW)F1 mice. *PLoS one*. 2009; 4(12):e8474. <https://doi.org/10.1371/journal.pone.0008474> PMID: 20041189; PubMed Central PMCID: PMC2793523.
30. Zykova SN, Tveita AA, Rekvig OP. Renal Dnase1 enzyme activity and protein expression is selectively shut down in murine and human membranoproliferative lupus nephritis. *PLoS one*. 2010; 5(8). <https://doi.org/10.1371/journal.pone.0012096> PMID: 20856893; PubMed Central PMCID: PMC2938370.
31. Bygrave AE, Rose KL, Cortes-Hernandez J, Warren J, Rigby RJ, Cook HT, et al. Spontaneous autoimmunity in 129 and C57BL/6 mice—implications for autoimmunity described in gene-targeted mice. *PLoS Biol*. 2004; 2(8):E243. <https://doi.org/10.1371/journal.pbio.0020243> PMID: 15314659.
32. Napirei M, Gultekin A, Kloeckl T, Moroy T, Frostegard J, Mannherz HG. Systemic lupus-erythematosus: Deoxyribonuclease 1 in necrotic chromatin disposal. *Int J Biochem Cell Biol*. 2006; 38(3):297–306. <https://doi.org/10.1016/j.biocel.2005.10.023> PMID: 16352456.
33. Rossaint J, Herter JM, Van Aken H, Napirei M, Doring Y, Weber C, et al. Synchronized integrin engagement and chemokine activation is crucial in neutrophil extracellular trap-mediated sterile inflammation. *Blood*. 2014; 123(16):2573–84. <https://doi.org/10.1182/blood-2013-07-516484> PMID: 24335230.
34. Felix J, Erbacher A, Breckler M, Herve R, Lemeiter D, Mannherz HG, et al. Deoxyribonuclease 1-Mediated Clearance of Circulating Chromatin Prevents From Immune Cell Activation and Pro-inflammatory Cytokine Production, a Phenomenon Amplified by Low Trap1 Activity: Consequences for Systemic Lupus Erythematosus. *Frontiers in immunology*. 2021; 12:613597. <https://doi.org/10.3389/fimmu.2021.613597> PMID: 33746957; PubMed Central PMCID: PMC7969502.
35. Kenny EF, Raupach B, Abu Abed U, Brinkmann V, Zychlinsky A. Dnase1-deficient mice spontaneously develop a systemic lupus erythematosus-like disease. *Eur J Immunol*. 2019; 49(4):590–9. <https://doi.org/10.1002/eji.201847875> PMID: 30758851.
36. Baron WF, Pan CQ, Spencer SA, Ryan AM, Lazarus RA, Baker KP. Cloning and characterization of an actin-resistant DNase I-like endonuclease secreted by macrophages. *Gene*. 1998; 215(2):291–301. [https://doi.org/10.1016/s0378-1119\(98\)00281-9](https://doi.org/10.1016/s0378-1119(98)00281-9) PMID: 9714828.
37. Napirei M, Ludwig S, Mezrhah J, Klockl T, Mannherz HG. Murine serum nucleases—contrasting effects of plasmin and heparin on the activities of DNase1 and DNase1-like 3 (DNase113). *FEBS J*. 2009; 276(4):1059–73. <https://doi.org/10.1111/j.1742-4658.2008.06849.x> PMID: 19154352.
38. Sisirak V, Sally B, D'Agati V, Martinez-Ortiz W, Ozcakar ZB, David J, et al. Digestion of Chromatin in Apoptotic Cell Microparticles Prevents Autoimmunity. *Cell*. 2016; 166(1):88–101. <https://doi.org/10.1016/j.cell.2016.05.034> PMID: 27293190; PubMed Central PMCID: PMC5030815.
39. Wilber A, O'Connor TP, Lu ML, Karimi A, Schneider MC. Dnase113 deficiency in lupus-prone MRL and NZB/W F1 mice. *Clin Exp Immunol*. 2003; 134(1):46–52. <https://doi.org/10.1046/j.1365-2249.2003.02267.x> PMID: 12974753.
40. Al-Mayouf SM, Sunker A, Abdwani R, Abrawi SA, Almurshedi F, Alhashmi N, et al. Loss-of-function variant in DNASE1L3 causes a familial form of systemic lupus erythematosus. *Nat Genet*. 2011; 43(12):1186–8. <https://doi.org/10.1038/ng.975> PMID: 22019780.
41. Jimenez-Alcazar M, Rangaswamy C, Panda R, Bitterling J, Simsek YJ, Long AT, et al. Host DNases prevent vascular occlusion by neutrophil extracellular traps. *Science*. 2017; 358(6367):1202–6. <https://doi.org/10.1126/science.aam8897> PMID: 29191910.
42. Jimenez-Alcazar M, Napirei M, Panda R, Kohler EC, Kremer Hovinga JA, Mannherz HG, et al. Impaired DNase1-mediated degradation of neutrophil extracellular traps is associated with acute thrombotic microangiopathies. *Journal of thrombosis and haemostasis: JTH*. 2015; 13(5):732–42. <https://doi.org/10.1111/jth.12796> PMID: 25418346.
43. Mizuta R, Araki S, Furukawa M, Furukawa Y, Ebara S, Shiokawa D, et al. DNase gamma is the effector endonuclease for internucleosomal DNA fragmentation in necrosis. *PLoS one*. 2013; 8(12):e80223. <https://doi.org/10.1371/journal.pone.0080223> PMID: 24312463; PubMed Central PMCID: PMC3846476.
44. Napirei M, Basnakian AG, Apostolov EO, Mannherz HG. Deoxyribonuclease 1 aggravates acetaminophen-induced liver necrosis in male CD-1 mice. *Hepatology*. 2006; 43(2):297–305. <https://doi.org/10.1002/hep.21034> PMID: 16440339.
45. Napirei M, Wulf S, Mannherz HG. Chromatin breakdown during necrosis by serum Dnase1 and the plasminogen system. *Arthritis Rheum*. 2004; 50(6):1873–83. <https://doi.org/10.1002/art.20267> PMID: 15188364.
46. Watanabe T, Takada S, Mizuta R. Cell-free DNA in blood circulation is generated by DNase1L3 and caspase-activated DNase. *Biochem Biophys Res Commun*. 2019; 516(3):790–5. <https://doi.org/10.1016/j.bbrc.2019.06.069> PMID: 31255286.

47. Basnakian AG, Apostolov EO, Yin X, Napirei M, Mannherz HG, Shah SV. Cisplatin nephrotoxicity is mediated by deoxyribonuclease I. *J Am Soc Nephrol*. 2005; 16(3):697–702. <https://doi.org/10.1681/ASN.2004060494> PMID: 15647342.
48. Shiokawa D, Ohyama H, Yamada T, Takahashi K, Tanuma S. Identification of an endonuclease responsible for apoptosis in rat thymocytes. *Eur J Biochem*. 1994; 226(1):23–30. <https://doi.org/10.1111/j.1432-1033.1994.tb20022.x> PMID: 7957253.
49. Mannherz HG, Peitsch MC, Zanotti S, Paddenberg R, Polzar B. A new function for an old enzyme: the role of DNase I in apoptosis. *Curr Top Microbiol Immunol*. 1995; 198:161–74. https://doi.org/10.1007/978-3-642-79414-8_10 PMID: 7774280.
50. Polzar B, Peitsch MC, Loos R, Tschopp J, Mannherz HG. Overexpression of deoxyribonuclease I (DNase I) transfected into COS-cells: its distribution during apoptotic cell death. *Eur J Cell Biol*. 1993; 62(2):397–405. PMID: 7925495.
51. Lazarides E, Lindberg U. Actin is the naturally occurring inhibitor of deoxyribonuclease I. *Proc Natl Acad Sci U S A*. 1974; 71(12):4742–6. <https://doi.org/10.1073/pnas.71.12.4742> PMID: 4140510.
52. Eulitz D, Mannherz HG. Inhibition of deoxyribonuclease I by actin is to protect cells from premature cell death. *Apoptosis*. 2007; 12(8):1511–21. <https://doi.org/10.1007/s10495-007-0078-4> PMID: 17468836.
53. Fahmi T, Wang X, Zhdanov DD, Islam I, Apostolov EO, Savenka AV, et al. DNase I Induces Other Endonucleases in Kidney Tubular Epithelial Cells by Its DNA-Degrading Activity. *International journal of molecular sciences*. 2020; 21(22). <https://doi.org/10.3390/ijms21228665> PMID: 33212932; PubMed Central PMCID: PMC7698339.
54. Higami Y, Tsuchiya T, To K, Chiba T, Yamaza H, Shiokawa D, et al. Expression of DNase gamma during Fas-independent apoptotic DNA fragmentation in rodent hepatocytes. *Cell Tissue Res*. 2004; 316(3):403–7. <https://doi.org/10.1007/s00441-004-0890-x> PMID: 15118903.
55. Brake AJ, Merryweather JP, Coit DG, Heberlein UA, Masiarz FR, Mullenbach GT, et al. Alpha-factor-directed synthesis and secretion of mature foreign proteins in *Saccharomyces cerevisiae*. *Proc Natl Acad Sci U S A*. 1984; 81(15):4642–6. <https://doi.org/10.1073/pnas.81.15.4642> PMID: 6087338; PubMed Central PMCID: PMC391546.
56. Chahal S, Wei P, Moua P, Park SP, Kwon J, Patel A, et al. Structural characterization of the alpha-mating factor prepro-peptide for secretion of recombinant proteins in *Pichia pastoris*. *Gene*. 2017; 598:50–62. <https://doi.org/10.1016/j.gene.2016.10.040> PMID: 27984193.
57. Brenner C, Fuller RS. Structural and enzymatic characterization of a purified prohormone-processing enzyme: secreted, soluble Kex2 protease. *Proc Natl Acad Sci U S A*. 1992; 89(3):922–6. <https://doi.org/10.1073/pnas.89.3.922> PMID: 1736307; PubMed Central PMCID: PMC48357.
58. Price PA, Liu TY, Stein WH, Moore S. Properties of chromatographically purified bovine pancreatic deoxyribonuclease. *J Biol Chem*. 1969; 244(3):917–23. PMID: 5769189.
59. Price PA, Stein WH, Moore S. Effect of divalent cations on the reduction and re-formation of the disulfide bonds of deoxyribonuclease. *J Biol Chem*. 1969; 244(3):929–32. PMID: 4976791.
60. Laemmli UK. Cleavage of structural proteins during the assembly of the head of bacteriophage T4. *Nature*. 1970; 227(259):680–5. <https://doi.org/10.1038/227680a0> PMID: 5432063.
61. Zacharius RM, Zell TE, Morrison JH, Woodlock JJ. Glycoprotein staining following electrophoresis on acrylamide gels. *Anal Biochem*. 1969; 30(1):148–52. [https://doi.org/10.1016/0003-2697\(69\)90383-2](https://doi.org/10.1016/0003-2697(69)90383-2) PMID: 4183001.
62. Kunitz M. Crystalline deoxyribonuclease; isolation and general properties; spectrophotometric method for the measurement of deoxyribonuclease activity. *J Gen Physiol*. 1950; 33(4):349–62. <https://doi.org/10.1085/jgp.33.4.349> PMID: 15406373; PubMed Central PMCID: PMC2147187.
63. Stolzenberg I, Wulf S, Mannherz HG, Paddenberg R. Different sublines of Jurkat cells respond with varying susceptibility of internucleosomal DNA degradation to different mediators of apoptosis. *Cell Tissue Res*. 2000; 301(2):273–82. <https://doi.org/10.1007/s004410000239> PMID: 10955723.
64. Kouyama T, Mihashi K. Fluorimetry study of N-(1-pyrenyl)iodoacetamide-labelled F-actin. Local structural change of actin protomer both on polymerization and on binding of heavy meromyosin. *Eur J Biochem*. 1981; 114(1):33–8. PMID: 7011802.
65. Qu Z, Fujita-Becker S, Ballweber E, Ince S, Herrmann C, Schroder RR, et al. Interaction of isolated cross-linked short actin oligomers with the skeletal muscle myosin motor domain. *FEBS J*. 2018; 285(9):1715–29. <https://doi.org/10.1111/febs.14442> PMID: 29575693.
66. Mannherz HG, Goody RS, Konrad M, Nowak E. The interaction of bovine pancreatic deoxyribonuclease I and skeletal muscle actin. *Eur J Biochem*. 1980; 104(2):367–79. <https://doi.org/10.1111/j.1432-1033.1980.tb04437.x> PMID: 6244947.
67. Miekka SI. Heat-induced fragmentation of human plasma fibronectin. *Biochim Biophys Acta*. 1983; 748(3):374–80. [https://doi.org/10.1016/0167-4838\(83\)90182-6](https://doi.org/10.1016/0167-4838(83)90182-6) PMID: 6196054.

68. Kowitz JD, Maloney J. Protein cleavage by boiling in sodium dodecyl sulfate prior to electrophoresis. *Anal Biochem.* 1982; 123(1):86–93. [https://doi.org/10.1016/0003-2697\(82\)90627-3](https://doi.org/10.1016/0003-2697(82)90627-3) PMID: 6810726.
69. Julius D, Schekman R, Thorner J. Glycosylation and processing of prepro-alpha-factor through the yeast secretory pathway. *Cell.* 1984; 36(2):309–18. [https://doi.org/10.1016/0092-8674\(84\)90224-1](https://doi.org/10.1016/0092-8674(84)90224-1) PMID: 6420074.
70. Yang Z, Zhang Z. Engineering strategies for enhanced production of protein and bio-products in *Pichia pastoris*: A review. *Biotechnology advances.* 2018; 36(1):182–95. <https://doi.org/10.1016/j.biotechadv.2017.11.002> PMID: 29129652.
71. Napirei M, Wulf S, Eulitz D, Mannherz HG, Kloeckl T. Comparative characterization of rat deoxyribonuclease 1 (Dnase1) and murine deoxyribonuclease 1-like 3 (Dnase1l3). *Biochem J.* 2005; 389(Pt 2):355–64. <https://doi.org/10.1042/BJ20042124> PMID: 15796714; PubMed Central PMCID: PMC1175112.
72. Zhu T, Guo M, Tang Z, Zhang M, Zhuang Y, Chu J, et al. Efficient generation of multi-copy strains for optimizing secretory expression of porcine insulin precursor in yeast *Pichia pastoris*. *Journal of applied microbiology.* 2009; 107(3):954–63. <https://doi.org/10.1111/j.1365-2672.2009.04279.x> PMID: 19486418.
73. Reverter D, Ventura S, Villegas V, Vendrell J, Aviles FX. Overexpression of human procarboxypeptidase A2 in *Pichia pastoris* and detailed characterization of its activation pathway. *J Biol Chem.* 1998; 273(6):3535–41. <https://doi.org/10.1074/jbc.273.6.3535> PMID: 9452479.
74. Miyajima A, Otsu K, Schreurs J, Bond MW, Abrams JS, Arai K. Expression of murine and human granulocyte-macrophage colony-stimulating factors in *S. cerevisiae*: mutagenesis of the potential glycosylation sites. *EMBO J.* 1986; 5(6):1193–7. PMID: 3525148; PubMed Central PMCID: PMC1166927.
75. Zsebo KM, Lu HS, Fieschko JC, Goldstein L, Davis J, Duker K, et al. Protein secretion from *Saccharomyces cerevisiae* directed by the prepro-alpha-factor leader region. *J Biol Chem.* 1986; 261(13):5858–65. PMID: 3009432.
76. Sola RJ, Griebenow K. Glycosylation of therapeutic proteins: an effective strategy to optimize efficacy. *BioDrugs: clinical immunotherapeutics, biopharmaceuticals and gene therapy.* 2010; 24(1):9–21. <https://doi.org/10.2165/11530550-000000000-00000> PMID: 20055529; PubMed Central PMCID: PMC2805475.
77. Sreenivas S, Krishnaiah SM, Govindappa N, Basavaraju Y, Kanojia K, Mallikarjun N, et al. Enhancement in production of recombinant two-chain Insulin Glargine by over-expression of Kex2 protease in *Pichia pastoris*. *Applied microbiology and biotechnology.* 2015; 99(1):327–36. <https://doi.org/10.1007/s00253-014-6052-5> PMID: 25239036.
78. Yang S, Kuang Y, Li H, Liu Y, Hui X, Li P, et al. Enhanced production of recombinant secretory proteins in *Pichia pastoris* by optimizing Kex2 P1' site. *PloS one.* 2013; 8(9):e75347. <https://doi.org/10.1371/journal.pone.0075347> PMID: 24069404; PubMed Central PMCID: PMC3777899.
79. Seeboth PG, Heim J. In-vitro processing of yeast alpha-factor leader fusion proteins using a soluble yscF (Kex2) variant. *Applied microbiology and biotechnology.* 1991; 35(6):771–6. <https://doi.org/10.1007/BF00169893> PMID: 1367896.
80. Garcia-Ortega X, Adelantado N, Ferrer P, Montesinos JL, Valero F. A step forward to improve recombinant protein production in *Pichia pastoris*: From specific growth rate effect on protein secretion to carbon-starving conditions as advanced strategy. *Process Biochemistry.* 2016; 51:681–91.
81. Vogl T, Glieder A. Regulation of *Pichia pastoris* promoters and its consequences for protein production. *New biotechnology.* 2013; 30(4):385–404. <https://doi.org/10.1016/j.nbt.2012.11.010> PMID: 23165100.
82. Krysan DJ, Ting EL, Abeijon C, Kroos L, Fuller RS. Yapsins are a family of aspartyl proteases required for cell wall integrity in *Saccharomyces cerevisiae*. *Eukaryotic cell.* 2005; 4(8):1364–74. <https://doi.org/10.1128/EC.4.8.1364-1374.2005> PMID: 16087741; PubMed Central PMCID: PMC1214537.
83. Cawley NX, Portela-Gomes G, Lou H, Loh YP. Yapsin 1 immunoreactivity in {alpha}-cells of human pancreatic islets: implications for the processing of human proglucagon by mammalian aspartic proteases. *The Journal of endocrinology.* 2011; 210(2):181–7. <https://doi.org/10.1530/JOE-11-0121> PMID: 21632904; PubMed Central PMCID: PMC3640344.
84. Egel-Mitani M, Flygenring HP, Hansen MT. A novel aspartyl protease allowing KEX2-independent MF alpha propheromone processing in yeast. *Yeast.* 1990; 6(2):127–37. <https://doi.org/10.1002/yea.320060206> PMID: 2183521.
85. Salamin K, Sriranganadane D, Lechenne B, Jousson O, Monod M. Secretion of an endogenous subtilisin by *Pichia pastoris* strains GS115 and KM71. *Applied and environmental microbiology.* 2010; 76(13):4269–76. <https://doi.org/10.1128/AEM.00412-10> PMID: 20472730; PubMed Central PMCID: PMC2897435.
86. Sinha J, Plantz BA, Inan M, Meagher MM. Causes of proteolytic degradation of secreted recombinant proteins produced in methylotrophic yeast *Pichia pastoris*: case study with recombinant ovine

- interferon-tau. *Biotechnology and bioengineering*. 2005; 89(1):102–12. <https://doi.org/10.1002/bit.20318> PMID: 15580575.
87. Fujihara J, Yasuda T, Kunito T, Fujii Y, Takatsuka H, Moritani T, et al. Two N-linked glycosylation sites (Asn18 and Asn106) are both required for full enzymatic activity, thermal stability, and resistance to proteolysis in mammalian deoxyribonuclease I. *Bioscience, biotechnology, and biochemistry*. 2008; 72(12):3197–205. <https://doi.org/10.1271/bbb.80376> PMID: 19060393.
 88. Campbell VW, Jackson DA. The effect of divalent cations on the mode of action of DNase I. The initial reaction products produced from covalently closed circular DNA. *J Biol Chem*. 1980; 255(8):3726–35. PMID: 6245089.
 89. Leppkes M, Knopf J, Naschberger E, Lindemann A, Singh J, Herrmann I, et al. Vascular occlusion by neutrophil extracellular traps in COVID-19. *EBioMedicine*. 2020; 58:102925. <https://doi.org/10.1016/j.ebiom.2020.102925> PMID: 32745993; PubMed Central PMCID: PMC7397705.
 90. Barnes BJ, Adrover JM, Baxter-Stoltzfus A, Borczuk A, Cools-Lartigue J, Crawford JM, et al. Targeting potential drivers of COVID-19: Neutrophil extracellular traps. *J Exp Med*. 2020; 217(6). <https://doi.org/10.1084/jem.20200652> PMID: 32302401; PubMed Central PMCID: PMC7161085.